# CHEMICAL ENGINEERING

November 2019

ESSENTIALS FOR THE CPI PROFESSIONAL

www.chemengonline.com

# Computational Fluid Dynamics

page 28

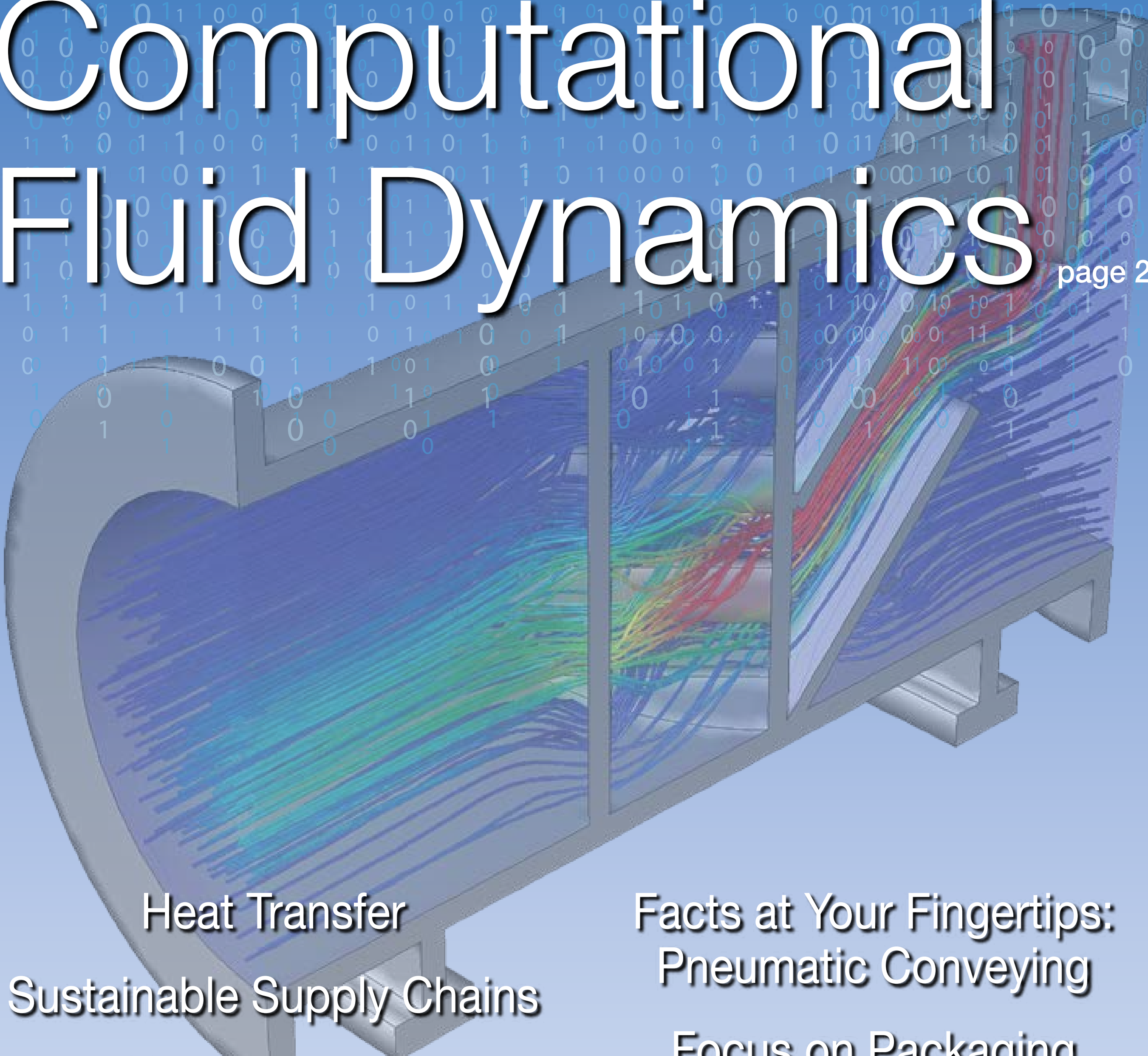

Heat Transfer

Sustainable Supply Chains

Water Treatment

Security Audits

Facts at Your Fingertips: Pneumatic Conveying

Focus on Packaging

Production of Nitrile Rubber

Access Intelligence

CHEMICAL ENGINEERING 11 COMPUTATIONAL FLUID DYNAMICS • HEAT TRANSFER VOL. 126 NO. 11 NOVEMBER 2019

CHEMICAL ENGINEERING
ESSENTIALS FOR THE CPI PROFESSIONAL

www.chemengonline.com

November 2019 Volume 126 | no. 11

## Cover Story

**28** **Part 1 CFD: Driving Engineering Productivity**
This article provides an overview of how computational fluid dynamics (CFD) works, and the benefits it brings to the chemical process industries

**33** **Part 2 Portable CFD: Building Interpolation Models from CFD Results**
Portable laptop computers and smartphones can be used to emulate CFD modeling results using this interpolation procedure

## In the News

**5** **Chementator**
A control valve with built-in flowmeter; Reducing emissions from carbon-fiber manufacturing; Converting hazardous phenols into luciferin; Symmetrical fuel-cell design simplifies $CO_2$ conversion; Modifying waste biomass to catalytically degrade pollutants; Making chemicals by artificial photosynthesis; and more

**10** **Business News**
Arkema to expand PVDF plant in Changsu; Arlanxeo invests in expansions for CR and NBR products; BASF to expand integrated ethylene oxide and derivatives complex in Antwerp; Wacker starts up pyrogenic silica plant in Tennessee; LyondellBasell expands PP compounding capacity in Germany; and more

**12** **Newsfront The New Era of Sustainable Supply Chains** To improve sustainability, materials manufacturers are welcoming new digital technologies and process innovations into their global supply chains

**16** **Newsfront Improved Water Treatment Technologies Make Waves** Greener chemistries and equipment advances provide more sustainable water-treatment options for chemical processors

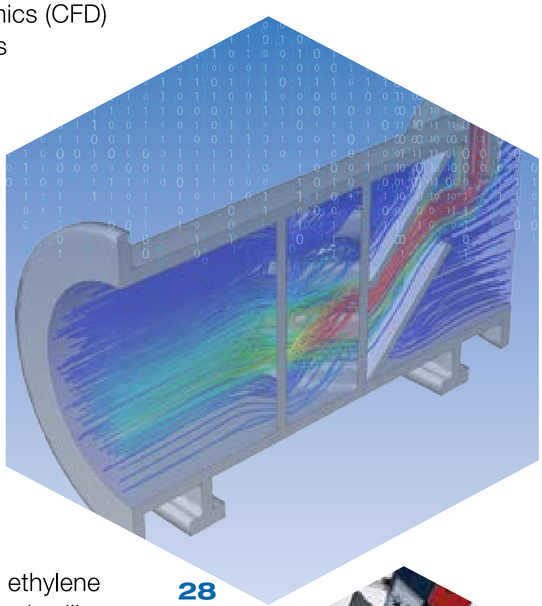

28

12

16

48

## Technical and Practical

**25** **Facts at your Fingertips Pneumatic Conveying: Pipeline Bend Challenges** This one-page reference reviews the potential problems that can arise from particle impacts in the pipe bends of dilute-phase pneumatic conveying systems

**26** **Technology Profile Production of Nitrile Rubber**
This column outlines a production process for the synthetic copolymer nitrile rubber, also known as Buna-N

**42** **Feature Report Part 1 Heat Exchangers: Design Considerations for SCF Service** Working with supercritical fluids (SCFs) poses challenges when designing heat exchangers. Some practical tips and precautions are presented here

**48** **Feature Report Part 2 ASTM Standards for Heat Transfer Fluids** This practical overview of ASTM standards can serve as a roadmap when selecting and evaluating heat transfer fluids


52

21

23

**52 Environmental Manager Preparing for a Successful Security Audit** Facing a site-security audit might seem daunting, but proper preparation will help to meet the goals of enhancing security and reducing risk

## Equipment and Services

**21 Focus on Packaging**
Label applicator with enhanced IoT capabilities; Vacuum technology for dust-free filling of fine powders; These load stops ensure perfect pallet placement; This packaging-line lift has an integrated scale and conveyor; This stacker features powered lift and drive; and more

**23 New Products**
This monitoring platform has built-in cybersecurity; Turbo blowers added to this company's product portfolio; New flow and energy meters for non-invasive measurements; These new drives feature enhanced safety functionality; New membrane elements tackle biofouling in desalination units; and more

## Departments

**3 Editor's Page Minimizing waste takes center stage**
Growing concerns about the impact of waste on our environment and corporate sustainability mandates are driving technological advances

**60 Economic Indicators**

## Advertisers

**40 Hot Products**
**56 Classified**
**58 Subscription and Sales Representative Information**
**59 Ad Index**

## Chemical Connections

**Follow @ChemEngMag on Twitter**

**Join the *Chemical Engineering* Magazine LinkedIn Group**

**Visit us on www.chemengonline.com for more articles, Latest News, Webinars, Test your Knowledge Quizzes, Bookshelf and more**

## Coming in December

Look for: **Feature Reports** on Cost Engineering; and Tanks & Vessels; A **Focus** on Valves; A **Facts at your Fingertips** on Agglomeration; **News Articles** on CPI Workforce Issues; and Simulation & Modeling Software ; **New Products**; and much more

**Cover imagery:** Some imagery for the cover was provided by Ansys Inc.
**Cover design:** Rob Hudgins

CHEMICAL ENGINEERING
ESSENTIALS FOR THE CPI PROFESSIONAL



# Editor's Page

## Minimizing waste takes center stage

Growing awareness of and concerns about the impact of waste on our environment, along with corporate directives to improve sustainability, are driving numerous initiatives that focus on recycling and other technologies for reducing waste. Many companies in the chemical process industries (CPI) have made commitments to develop more sustainable practices and are reporting on their progress.

### Reducing plastic waste

Plastic waste has garnered particular attention and commitments from CPI companies, including the ambitious goal of eliminating plastic waste*. Mentioned here are some recent developments, several of which were announced at last month's show for plastics and rubbers, K 2019 (Düsseldorf, Germany; October 16 to 23), where reducing plastic waste was a major topic.

Mitsui Chemicals, Inc. (www.mitsuichem.com) is collaborating with Kaisei Inc. to commercialize bio-polypropylene. The method being investigated would ferment mainly non-edible biomass to produce isopropanol, which would be dehydrated to obtain propylene.

BASF (www.basf.com) is investing €20 million in Quantafuel, a specialist in the pyrolysis of mixed plastic waste and purification of pyrolysis oil. The intention is to develop technology for chemical recycling and use the recycled product as feedstock in chemical production. BASF's ChemCycling project aims to process recycled raw materials obtained from plastic waste. Prototypes based on chemically recycled plastic waste, including food packaging, have already been made.

SABIC (www.sabic.com) highlighted several of its sustainable technologies at K 2019, including its "certified circular polymers" that are created from chemically recycled mixed plastic waste. The company's Trucircle initiative includes certified renewable polyethylene and polypropylene, and polymer resins created from mechanically recycled polymers.

Clariant (www.clariant.com ) introduced its EcoCircle Centers of Excellence, for collaborative research and joint development of products for a circular plastics economy. Projects on mechanical recycling of packaging materials are said to be underway. Future facilities will include a mini recycling plant for polyolefins and supporting laboratory capabilities.

Baerlocher (www.baerlocher.com), a supplier of plastic additives, offers a proprietary Resin Stabilization Technology (RST) that aims to improve quality and consistency issues that result from using recycled plastics. The company reports that its RST stabilizers enable manufacturers to increase the use of recycled plastic waste in their products.

### Beyond plastics

Waste reduction technologies are being developed for much more than plastics. One example is a recent announcement by AkzoNobel (www.akzonobel.com), that it is the first major manufacturer to launch recycled paints. In partnership with Veolia, AkzoNobel is creating a product called Evolve Matt, which is part of its Dulux Trade brand, that contains 35% recycled paint.

The initiatives mentioned here represent only a fraction of the work being pursued on sustainability within the CPI. Further developments in technologies for sustainability can be found in this issue — in the Newsfronts on supply chains (pp. 12–14), and on water treatment (pp. 16–20), as well as in our Chementator department (pp. 5–9). ■

*Dorothy Lozowski, Editorial Director*

* www.chemengonline.com/ending-plastic-waste/

## A control valve with built-in flowmeter

On September 19, Focus-On (Dordrecht, the Netherlands; www.focus-on-process.com) — a new, 50:50 joint-venture (JV) of Samson AG (Frankfurt am Main; www.samson.de) and Krohne GmbH & Co. KG (Duisburg, both Germany; www.krohne.com) — introduced its new "intelligent process node," a device that combines three functions: sensor, actuator and control. The module incorporates an ultrasonic flow sensor to measure flow in a pipeline and regulates its valve function independently using adaptive control to achieve specific set points. In addition to flow, the module also measures temperature and pressure (including differential pressure). This feature, combined with integrated diagnostics functions and artificial intelligence, enables the autonomous actuator to know its current status, predict its future conditions, and learn to adapt to specific applications. The device can, for example, recognize and predict cavitation. The increased stress and wear of the valve and piping can be avoided or significantly reduced, says the company.

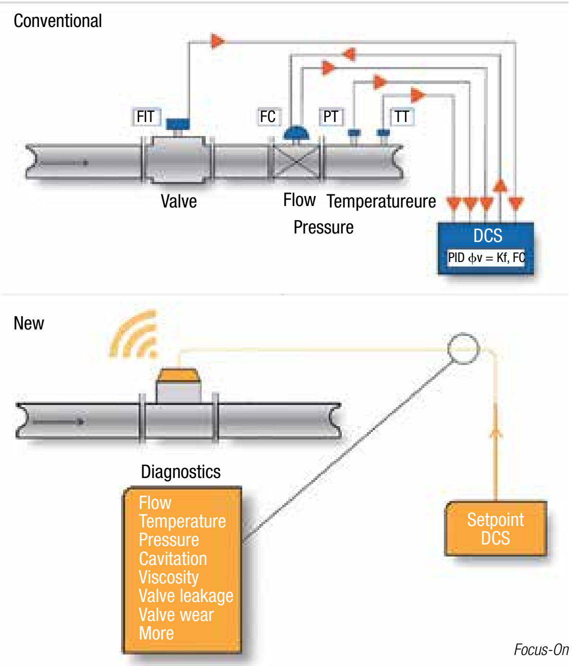

Focus-On

Integrated into the device is a digital twin, which can generate model data and compare actual with virtual data (temperature, pressure and flowrate) in the virtual world, and generate data for predicting failure. "The difference here is that the digital twin is not in 'the cloud,' but in the device itself — this is a first," says Focus-On managing director André Boer. Because all sensors, control and actuator are integrated into a single device, cycle times can be up to ten times faster than conventional systems. "This allows for better control, without overshoot," he says.

Capital expenditures for using the device are said to be reduced by at least 33%, compared to a conventional setup with a control valve and separate sensors for flow, temperature and pressure. "The cost savings are due to having one specification sheet instead of four, two flanges instead of six or seven, and less piping. The space savings is especially attractive for builders of skid-mounted units, where space is at a premium. Fewer flanges also means a lower risk of leaks," says Focus-On managing director Kavreet Bhangu.

Five test units are now being tested by Krohne in Duisburg, and another five by Samson in Frankfurt. Field trials will begin in the next several weeks. Focus-On plans to launch a first commercial product in the first quarter of 2020. This will be a unit with DN 80 (3-in.) flange size, PN 16/40 — Class 150/300 pressure rating for non-Ex applications. Ex certification is underway. Smaller and larger sizes will be released later in 2020.

Edited by:
**Gerald Ondrey**

### NATURAL WAX COATING

Researchers from Aalto University (Finland; www.aalto.fi) have developed a new way of making garments water-resistant, without using toxic chemicals. The treatment is non-toxic, and does not impair breathability.

The coating uses carnauba wax from Brazilian palm-tree leaves. This wax is already used in medicines and foodstuffs, as well as the surface treatment of fruits and car waxes. During the processing, the wax is thawed and decomposed in water into wax particles that are anionic, just like cellulose. For the wax particles to adhere well to the cellulose surface, something cationic is needed as a buffer. In previous studies, a natural protein called polylysine was used for this. However, as doctoral student Nina Forsman points out, "polylysine is very expensive, so in our current study, it's been substituted with a much cheaper, cationic starch that's already commercially available." Though cationic starch is not quite as effective as polylysine, two layers of the starch mixed with two wax particles are sufficient to make the textile waterproof.

The wax coating can be

(Continues on p. 6)

## Reducing emissions from carbon-fiber manufacturing

Carbon fibers are typically fabricated by the oxidation of a polymeric fiber, such as polyacrylonitrile (PAN) at 200–300°C, which generates a large amount of exhaust air containing several hundred parts per million (ppm) of hydrogen cyanide and ammonia. This is followed by a carbonization process at 1,000–1,200°C, which takes place under an inert atmosphere, such as $N_2$. The second step generates a smaller amount of exhaust $N_2$, but with high concentrations of HCN and $NH_3$. Conventional treatment systems are unable to handle both the destruction of HCN and $NH_3$ emissions while suppressing the generation of oxides of nitrogen (NOx).

To solve this problem, Taiyo Nippon Sanso Ltd. (Tokyo, Japan; www.tn-sanso.co.jp) has developed a system called Innova-Flash, which uses a two-step oxidation process to treat both exhaust streams. In the first step, the highly concentrated HCN/$NH_3$-laden $N_2$ undergoes a high-temperature treatment under reductive conditions. In the second step, a low-temperature oxidation process removes the low concentration of HCN and $NH_3$ in the air exhaust. By injecting the combustion gas (which also contains fuel components) generated in the first step into the second step, energy savings of approximately 50% are achieved, says the company.

Tests with Innova-Flash have confirmed that NOx emissions from the concentrated stream are suppressed to below 100 ppm, and to below 40 ppm from the low-concentration exhaust stream.

applied to the textile by dipping, spraying or brushing onto the surface of the textile. In industrial-scale production, wax treatment could be part of the textile finishing process along with the color pigmentation of the wax, which makes dyeing and waterproofing possible at the same time.

## BIOMASS UTILIZATION

Startup company CH-Bioforce Oy (Espoo, Finland; www.ch-bioforce.com) has developed a "breakthrough technology" that allows the efficient extraction of lignocellulosic biomass constituents in an economically sound way, with extremely high purity, and on an industrial scale. The technology produces high-quality biopolymers — high-purity pulp, polymeric hemicellulose and sulfur-free lignin. Each of these material streams has a wide range of possible end applications, especially in replacing fossil-based materials and less environmentally friendly bio-based products, such as food-based starch or cotton.

CH-Bioforce's technology is able to utilize over 90% of biomass, compared to less than 50% utilization commonly achieved in a biorefinery, the company says. And none of the current alternative methods can fractionate all of the constituents in one process. Also, the new technology can utilize almost any kind of biomass as feedstock: wood, such as birch, pine and spruce; and also non-wood, such as straw and bagasse, which are not suitable for commonly used pulping processes.

The technology is already in place, has been widely tested and is ready to be scaled up to industrial level.

## STORING HEAT

Since July, a full-scale demonstration of an energy-storage system that captures low-temperature (less than 100°C) exhaust heat has been underway in a project led by the New Energy and Industrial Technology Development Organization (NEDO; Kawasaki City, Japan; www.nedo.go.jp). Together with five industrial partners, the National Institute of Advanced Industrial Science and Technology (AIST) and Hamura City Local Government, NEDO will be testing the heat-

(Continues on p. 7)

# A new platform for atmospheric monitoring

Scientists at Nanyang Technological University (NTU; Singapore; www.ntu.edu.sg) have developed a device that can identify a wide range of airborne gases and chemicals instantly. The prototype device is portable and suitable for rapid deployment by agencies to identify airborne hazards, such as sulfur dioxide and benzene. It can provide realtime monitoring of air quality, as well as detecting gas leaks and industrial air pollution.

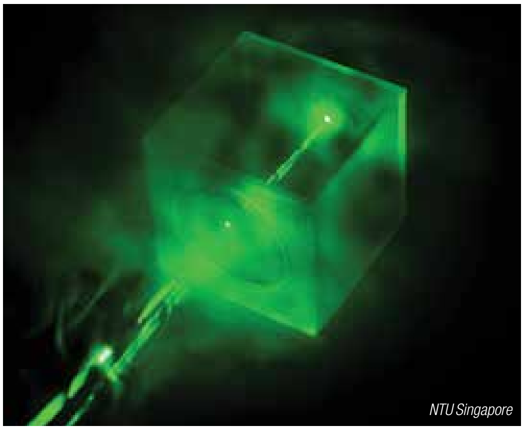

*NTU Singapore*

Developed by a research team led by associate professor Ling Xing Yi at the School of Physical and Mathematical Sciences, the new technology was reported in the September 19 issue of *ACS Nano*.

The device is based on the principle of stand-off Raman spectroscopy (SORS), which combines the advantages of both Raman spectroscopy and remote detection to identify chemicals at inaccessible sites. Although SORS is not new, the method has been limited to the detection of pure liquids and solids due to the low concentrations of molecules that are dispersed in air. To overcome this limitation, the researchers developed a highly porous metal-organic framework (MOF) that actively absorbs and traps molecules from the air into a "cage." Formed by the self-assembly of Ag@MOF core-shell nanoparticles, the 3-D "plasmonic architecture" exhibits a micrometer-thick surface-enhanced Raman scattering (SERS) hotspot, whereby the metal nanoparticles essentially boost the intensity of the light surrounding the molecules. This results in a million-fold enhancement in the Raman signals, enabling a rapid detection of aerosols, gas, and volatile organic compounds (VOCs) down to parts-per-billion levels at a distance of up to 10 m, the scientists report. A measurement and identification takes about 10 s to complete.

Through the university's innovation and enterprise company, NTUitive, the team has filed for a patent and is now commercializing the technology.

# Rechargeable $MnO_2$-Zn batteries with a higher voltage

Researchers at the City University of New York Energy Institute (ccny.cuny.edu) have developed a low-cost battery based on manganese dioxide and zinc that reaches voltages of greater than 2 V, a first-time achievement that could allow batteries with these low-cost raw materials to compete with lithium-ion batteries.

Alkaline $MnO_2$/Zn batteries are familiar as primary (one-time discharge) batteries for small electronics, but they generate low (1.2 V) voltages because both the cathode and anode reactions occur in alkaline electrolyte. The CCNY research group has designed Zn/Mn batteries with both reversibility and higher voltage.

Previous attempts to raise the voltage of the system thermodynamically has involved separating electrolytes with ceramic or ion-selective membranes so that the anode reaction occurs in alkaline conditions and the cathode half-reaction in acid environs. However, the membranes push the battery's costs too high to compete with existing alternatives.

The CCNY team, led by professor Gautam Yadav, invented a novel way to separate the battery half-cells by engineering the alkaline electrolyte into a thick gel whose interfacial properties prevent it from mixing with the liquid acidic solution and undergoing neutralization reactions. "There is an ionic barrier that prevents the electrolytes from neutralization and allows the battery to maintain a high voltage. By utilizing this procedure, we were able to successfully move away from expensive membranes, which can stifle a new battery from entering into the market," Yadav says.

Yadav's team built a rechargeable battery cell that mimics the size and shape of commercially available AA and D cell primary batteries. The group is designing the batteries for portable electronics, e-bikes and other applications where energy density, cost and safety are paramount, Yadav says.

## Converting hazardous phenols into luciferin

Phenolic compounds, such as chloro- and nitrophenols, are potentially hazardous when found in soils and the workplace. Normally, such compounds are detected with techniques such as mass spectrometry. There are several mechanisms for degrading and detoxifying contaminants: bacteria use specialized enzymes to dehalogenate phenols and convert them to oxidized compounds called benzoquinones, which can be metabolized by organisms. Enzymes such as dehalogenases or mono-oxygenases have been used in industry for biological detoxification. Now, researchers from Thailand have gone further than just detoxification, and coupled the enzymatic process with a method to convert the benzoquinone into luciferin — the substance that causes the glowing of fireflies.

The researchers, from the Vidyasirimedhi Institute of Science and Technology (Rayong, Thailand; www.vistec.ac.th), led by professor Pimchai Chaiyen, say the chemoenzymatic cascade entails conversion of the product from the first enzymatic conversion step, benzoquinone, into luciferin in a second step, but within the same reaction vessel.

To achieve conversion of benzoquinone to luciferin, the researchers add the natural compound cysteine to the reaction mixture. They then include a third step in the reaction sequence and detect the luciferin through the glowing reaction caused by the enzyme luciferase, which is also present in fireflies. They also proved that their combined method of both the detoxification and the luciferin production and detection is robust and capable of quantitative conversion of hazardous phenols to luciferin.

Their method — the simultaneous detoxification and luciferin production — offers additional benefits: luciferin is a valued compound in biomedicine. The method can also be used to synthesize luciferin from waste chemicals.

storage materials through February 2020. The high-performance and highly durable heat-storage materials, which can store more than twice the heat per unit volume compared to existing latent-heat storage materials were developed by AIST based on the desiccant Hasclay, which is named after the raw materials used to make it — hydroxyl aluminum silicate and clay.

The one-year demonstration, using 12 tons of Hasclay, involves two types of systems: an off-line heat transport-type system and a stationary-type system. For the first type, the exhaust heat generated at the cogeneration plant of Hakui Factory of Hino Motors Ltd. is to be stored in an off-line heat-transport system, and will then be used at both the air-conditioning facility within the factory and also to warm the swimming pool of Hakui City swimming center. Because the two locations are 2 km away from the factory, the heated storage material will be transported by a trailer. For the second type of application, the heat generated from a high-temperature

(Continues on p. 8)

titanium-oxide drying process at the Yokkaichi factory of Ishihara Sangyo Kaisha Ltd., will be stored and used to warm the low-temperature $TiO_2$.

### ETERNAL BIOCATALYSTS

Efficient catalysts for converting $H_2$ into electricity in fuel cells are often based on expensive, precious metals, such as platinum. Alternative catalysts based on less expensive metals or biological components may work just as efficiently, but have a short service due to sensitivity to oxygen. A research team, led by professor Nicolas Plumeré from the Ruhr Explores Solvation (Resolv) Cluster of Excellence at Ruhr-Universität Bochum (RUB; Germany: www.rub.de), with Vincent Fourmond and Christophe Léger from the Centre national de la recherche scientifique Marseille (CNRS; France; www.cnrs.fr), has succeeded in integrating such a catalyst within an extremely thin protective film of molecular building blocks that shields it from $O_2$, and thus makes its service life practically infinite while maintaining its ability to work efficiently.

Although protective films had been developed previously, they were found to be unsuitable for catalyst applications because the films were so thick (>100 µm), they hampered efficiency, says Plumeré.

In the current work, reported in the September 19 issue of *J. Am. Chem. Soc.*, the researchers show that, even in a much thinner polymer film, hydrogenase enzymes are safe from $O_2$. "Surprisingly, these films, which are only a few

(Continues on p. 9)

## Symmetrical fuel-cell design simplifies $CO_2$ conversion

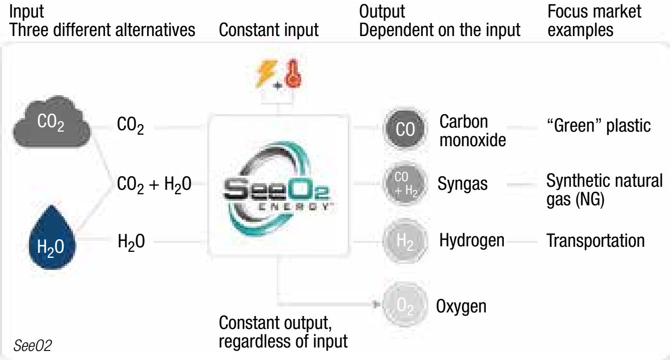


A new carbon-utilization technology developed by SeeO2 Energy Inc. (Calgary, Alta., Canada; www.seeo2energy.com) takes advantage of thermodynamics in a high-temperature electrolyzer to efficiently convert carbon dioxide into CO and $O_2$ with 100% selectivity. Based on the principle of a reversible solid-oxide fuel cell, the technology employs a perovskite-based catalyst that can withstand not only high temperatures and impurities, such as sulfur, without coking or decomposition, but also enables symmetrical operation on both sides of the electrochemical cell, explains Beatriz Molero Sanchez, SeeO2 co-founder and chief technology officer. "Normally, there would be one material for the electrode on each side of the cell. Our catalyst allows us to have a symmetrical design to make the fabrication process easier and less expensive," says Molero Sanchez. Beyond $CO_2$, SeeO2's cell can also electrolyze water, and can co-electrolyze water and $CO_2$ into syngas and $O_2$.

For scaleup purposes, however, the company is focusing on processing $CO_2$ streams — the technology has demonstrated effectiveness with high-purity $CO_2$, as well as streams with just 30% $CO_2$ content. Operating at high temperatures avoids some of the disadvantages of other $CO_2$-conversion processes, including catalyst poisoning, delamination within the cell and low selectivity. "At high currents, with some catalysts, the electrolyte and electrode physically separate and the device goes into failure mode. This catalyst provides a stable interface between the electrode and the electrolyte, and provides both electronic and ionic catalytic activity," adds Molero Sanchez.

SeeO2 was established in April 2018 and since then, it has developed a prototype unit that can convert 10 kg/d of $CO_2$. The company is currently working with Equinor ASA (Stavanger, Norway; www.equinor.com) to accelerate the technology, and plans are in place with Calgary-based energy company ATCO Ltd. to launch a pilot project in 2020. In preparation for commercialization, SeeO2 is also verifying the technology's use with direct fluegas streams to prove that impurities do not hinder $CO_2$ conversion. "Our next milestone is to field test the prototype in the real world. That's our stepping stone to commercial units that convert 1–3 ton/d of $CO_2$, with eventual plans to scale up to larger-capacity units in the range of 1,000 ton/d," adds Molero Sanchez.

## Modifying waste biomass to catalytically degrade pollutants

Sewage and wastewater often contain pollutants and environmental hormones (endocrine disruptors) that can have a negative effect on the environment and on human health. Catalysts currently used to destroy such pollutants involve high costs. And up to now, research has mostly focused on developing single-substance catalysts and enhancing their performance. Little research has been done to develop an eco-friendly nanocomposite catalyst capable of removing environmental hormones from sewage and wastewater.

Now a research team from the Korea Institute of Science and Technology (KIST; Seoul, South Korea; https://eng.kist.re.kr), led by Jae-woo Choi and Kyung-won Jung, has utilized biochar created from rice hulls to produce an eco-friendly, low-cost and highly efficient catalyst. They coated the surface of the biochar with nano-sized manganese dioxide to create a nanocomposite.

To make the catalyst, the KIST team used a hydrothermal method — a type of synthesis that uses high heat and pressure — to produce a nanocomposite. The team observed that giving the catalyst a three-dimensional, stratified structure resulted in the high effectiveness of the advanced oxidation process, due to the large surface area created.

The catalyst developed at KIST removed more than 95% of bisphenol A, an environmental hormone disruptor, in less than one hour, compared with 80% removal by the catalyst currently used. When combined with sonication (20 kHz ultrasound), the KIST catalyst removed all traces of bisphenol A in less than 20 min. Even after many repeated tests, the bisphenol A removal rate remained at about 93%.

# Making chemicals by artificial photosynthesis

Last month, Evonik Industries AG (Essen, Germany; www.evonik.com) and Siemens AG (Munich, both Germany; www.siemens.com) launched a second phase of their joint research project, Rheticus II, which aims to develop a test plant that will use $CO_2$ and water, as well as electricity from renewable sources and bacteria, to produce specialty chemicals. In the Rheticus I project, Siemens and Evonik worked for two years to develop the technically feasible basis for artificial photosynthesis using a bioreactor and electrolyzers (see "Solar Chemistry Heats Up," *Chem. Eng.*, March 2018, pp. 12–16). Now, the two companies are combining these two, previously separate, plants in a test facility at Evonik's site in Marl, Germany. Rheticus II will run until 2021 and will receive funding of around €3.5 million from Germany's Federal Ministry of Education and Research (BMBF; Bonn; www.bmbf.de).

The test facility is scheduled to start operating in early 2020. It comprises electrolyzers and a bioreactor. In a first step, $CO_2$ and water are electrolyzed into synthesis gas (syngas; CO and $H_2$). Microorganisms then metabolize the syngas into chemicals.

The synthesis module came on stream at Evonik in spring 2019. At its heart is an 8-m-high stainless-steel, 2,000-L bioreactor, which operates continuously. Siemens has developed a fully automated $CO_2$ electrolyzer, which was integrated into a container in summer 2019. The world's first $CO_2$ electrolyzer comprises ten cells, and the total surface area of the electrodes is 3,000 $cm^2$.

In the test facility, bacteria will produce butanol and hexanol for research purposes. These substances are used as starting products, for example, for specialty plastics and food supplements. However, other specialty chemicals are conceivable, depending on the bacterial strain and conditions, says Evonik.

Another advantage of Rheticus is that the technology platform also contributes to the reduction of carbon dioxide levels in the atmosphere, as it uses $CO_2$ as a raw material. Three tons of $CO_2$ would be needed to produce one ton of butanol, for example. ■

micrometers thick, are even more robust than the thicker ones," says Plumeré — 50% of the catalyst is utilized compared to only 0.3% for thicker protective films.

To make the films, the researchers use tiny (5-nm dia.) spheres that have an identical structure, known as dendrimers. This allowed the researchers to precisely control the thickness of the resulting layer. The dendrimers can transport electrons more efficiently than the polymers used previously. "This increased conductivity means that the electrons move more quickly through the film and are able to stop $O_2$ at a greater distance away from the catalyst," explains Plumeré.

The thickness of the protective film has a significant effect on the service life of the catalyst: In a 3-µm-thick film, a catalyst survives in the presence of $O_2$ for only around 10 min. If the film is 6-µm thick, the service life can be extended to up to 1 yr under the same conditions. "A further 2 µm in thickness theoretically extends the life of the catalyst to 22,000 years," say the researchers. ❑

## LINEUP

ADNOC
AMG
ARKEMA
ARLANXEO
BASF
DUPONT
ENTERPRISE PRODUCTS
LYONDELLBASELL
MARATHON PETROLEUM
MEGLOBAL
OCI
REPSOL
SHELL
SK GLOBAL CHEMICAL
SYNTHOMER
TORAY
TRINSEO
WACKER

Look for more latest news on chemengonline.com

## Plant Watch

**Arkema to expand PVDF plant in Changshu**

October 15, 2019 — Arkema (Colombes, France; www.arkema.com) will increase the capacity of polyvinylidene difluoride (PVDF) at its Changshu, China plant by approximately 50%. The expanded capacity is scheduled to come on stream in the fourth quarter of 2020.

**MEGlobal's U.S. Gulf Coast production plant officially starts up**

October 15, 2019 — The Equate Group (Al Ahmadi, Kuwait; www.equate.com) announced the startup of the MEGlobal Oyster Creek site in Texas. The site has achieved commercial production of fiber-grade monoethylene glycol. The plant has a capacity of 750,000 metric tons per year (m.t./yr).

**Arlanxeo invests in expansions for CR and NBR products**

October 10, 2019 — Arlanxeo Holding B.V. (Maastricht, the Netherlands; www.arlanxeo.com) completed a turnaround at its chloroprene rubber (CR) plant in Dormagen, Germany, allowing for production of up to 70,000 m.t./yr of CR. In addition to its investment in Dormagen, Arlanxeo has also already made substantial progress modernizing its nitrile butadiene rubber (NBR) plant in La Wantzenau, France.

**Trinseo to build thermoplastic elastomer pilot plant in Taiwan**

October 7, 2019 — Trinseo (Berwyn, Pa.; www.trinseo.com) plans to build a thermoplastic elastomers (TPE) pilot facility at the company's existing manufacturing site in Hsinchu, Taiwan. Once the new pilot line in Hsinchu is operational in 2020, Trinseo will locally produce TPE and thermoplastic urethanes (TPU), including its bioplastics portfolio.

**Wacker starts up pyrogenic silica plant in Tennessee**

October 3, 2019 — Wacker Chemie AG (Munich, Germany; www.wacker.com) brought a pyrogenic-silica manufacturing plant on stream at its site in Charleston, Tenn. The facility has a production capacity of 13,000 m.t./yr. Investments for the new facility total around $150 million. Pyrogenic silica is a formulation component for manufacturing silicone rubber.

**Enterprise Products to build new PDH plant with LyondellBasell propane supply**

October 2, 2019 — LyondellBasell Industries N.V. (Rotterdam, the Netherlands; www.lyondellbasell.com) and Enterprise Products Partners L.P. (Houston; www.enterpriseproducts.com) announced that their respective affiliates have executed longterm contracts that support construction of Enterprise's second propane dehydrogenation (PDH) plant (PDH 2). PDH 2 will have the capacity to consume up to 35,000 barrels per day (bbl/d) of propane and produce up to 1.65 billion pounds per year of polymer-grade propylene. PDH 2 will be located at Enterprise's complex in Mont Belvieu, Tex. The facility is scheduled to begin service in the first half of 2023.

**Toray starts production of PA and PBT at new compounding plant in India**

October 2, 2019 — Toray Industries, Inc. (Tokyo, Japan; www.toray.com) announced that its subsidiary in India, Toray Industries (India) Ltd., began manufacturing polyamide (PA) and polybutylene terephthalate (PBT) at a new facility. This new plant has a full operating capacity of around 5,000 m.t./yr.

**BASF to expand integrated ethylene oxide and derivatives complex in Antwerp**

September 30, 2019 — BASF SE (Ludwigshafen, Germany; www.basf.com) will expand the capacity of ethylene oxide (EO) and ethylene oxide derivatives (EOD) at its Verbund site in Antwerp, Belgium. The total investment adds about 400,000 m.t./yr to BASF's production capacity for the corresponding products with an expected investment amount exceeding €500 million. The project includes additional investments in several EOD plants producing non-ionic surfactants, glycol ethers and various other downstream alkoxylates.

**Synthomer inaugurates acrylic dispersions plant**

September 27, 2019 — Synthomer plc (London, U.K.; www.synthomer.com) inaugurated an expansion to its acrylic-dispersions production facility in Worms, Germany, increasing the site's capacity by 36,000 m.t./yr. The fully automated production facility significantly enhances the site's capability to produce made-to-order specialty acrylics.

**LyondellBasell expands PP compounding capacity in Germany**

September 26, 2019 — LyondellBasell started up the fifth production line at its Knapsack, Germany site, making Knapsack the world's largest polypropylene (PP) compounding facility. The new total annual production capacity for the site is more than 200,000 m.t./yr, with the new line's added capacity of 25,000 m.t./yr.

## Mergers & Acquisitions

**Arkema to divest Functional Polyolefins business to SK Global Chemical**

October 15, 2019 — Arkema announced the proposed divestment of its Functional Polyolefins business to SK Global Chemical

Co. (Seoul, South Korea; eng.skglobalchemical.com). The acquisition offer is based on an enterprise value of €335 million. The proposed transaction is expected to be finalized in the second quarter of 2020.

**Shell and AMG form JV for catalyst recycling**

October 14, 2019 — AMG Advanced Metallurgical Group N.V. (Amsterdam, the Netherlands; www.amg-nv.com) and Shell Catalysts & Technologies (www.shell.com/ct) have signed an agreement to form a joint venture (JV) called Shell & AMG Recycling B.V., which will focus on sustainable solutions for catalyst reclamation and recycling. The process employed by Shell & AMG Recycling B.V. extracts critical materials, including vanadium, in the form of ferrovanadium, from spent catalysts.

**Marathon Petroleum merges ethanol assets with Andersons**

October 3, 2019 — The Andersons, Inc. (Maumee, Ohio; www.andersonsinc.com) and Marathon Petroleum Corp. (Findlay, Ohio; www.marathompetroleum.com) have merged four ethanol entities into the new legal entity The Andersons Marathon Holdings LLC (TAMH). The ethanol facilities involved in the merger include those in Albion, Mich.; Clymers, Ind.; and Greenville, Ohio, which were all previously jointly owned by The Andersons and Marathon Petroleum; and The Andersons' wholly owned ethanol facility in Denison, Iowa.

**Repsol acquires stake in Singapore-based lubricants manufacturer**

October 1, 2019 — Repsol S.A. (Madrid, Spain; www.repsol.com) signed a purchase agreement for a 40% stake in the Singapore-based lubricants manufacturer United Oil Co., which will manufacture and supply Repsol products in Singapore, Indonesia, Malaysia and Vietnam. United Oil has two lubricants plants, in Singapore and Indonesia, with total capacity of 140,000 m.t./yr.

**ADNOC and OCI form fertilizer joint venture**

October 1, 2019 — OCI N.V. (Amsterdam, the Netherlands; www.oci.nl) and Abu Dhabi National Oil Co. (ADNOC; www.adnoc.com) have fully combined ADNOC's fertilizer business into OCI's Middle East and North Africa (MENA) nitrogen fertilizer platform, creating a new JV named Fertiglobe. Fertiglobe will be the largest fertilizer producer in the MENA region with annual production capacities of 5 million m.t. of urea and 1.5 million m.t. of ammonia.

**BASF to sell its ultrafiltration-membrane business to DuPont**

September 23, 2019 — BASF SE (Ludwigshafen, Germany; www.basf.com) will sell its ultrafiltration-membrane business to DuPont (Wilmington, Del.; www.dupont.com). The divesture includes the shares of inge GmbH, the business' international sales force and its headquarters and production site in Greifenberg, Germany. DuPont also recently announced the acquisition of Memcor ultrafiltration and membrane biofiltration technologies from Evoqua Water Technologies Corp. ■

*Mary Page Bailey*

# The New Era of Sustainable Supply Chains

**To improve sustainability, materials manufacturers are welcoming new digital technologies and process innovations into their global supply chains**

From palm oil to plastics, the global supply chains of many critical raw materials are evolving as consumers and manufacturers increasingly seek sustainable and renewable options. Digital technologies, including blockchain, Internet of Things (IoT) sensors and modeling tools, are facilitating these supply-chain transitions by enabling unprecedented data visibility and analyses. At the same time, chemical manufacturers are turning toward process and chemistry innovations to improve the sustainability of their raw materials.

## Blockchain delivers accountability

Blockchain, in particular, provides many specific capabilities that are helping manufacturers realize more sustainable sourcing practices. In the plastics sector, for instance, DOMO Chemicals (Ghent-Zwijnaarde, Belgium; www.domochemicals.com) and Covestro AG (Leverkusen, Germany; www.covestro.com), along with the Circularise initiative (www.circularise.com/plastics), are partnering to implement blockchain technology to improve traceability and transparency in plastics manufacturing. "Blockchain can be applied to many challenges in the plastics value chain, such as complex record keeping and tracking of products. Blockchain serves as a less corruptible and better automated alternative to centralized databases," says Jordi de Vos, founder of Circularise. Blockchain provides encoded information storage on a network-to-network chain, which validates data to protect business dealings and prevents the theft or manipulation of documents — a unique combination of transparency and security.

*Circularise*

**AN OPEN STANDARD FOR SUSTAINABILITY AND TRANSPARENCY IN THE PLASTICS INDUSTRY**

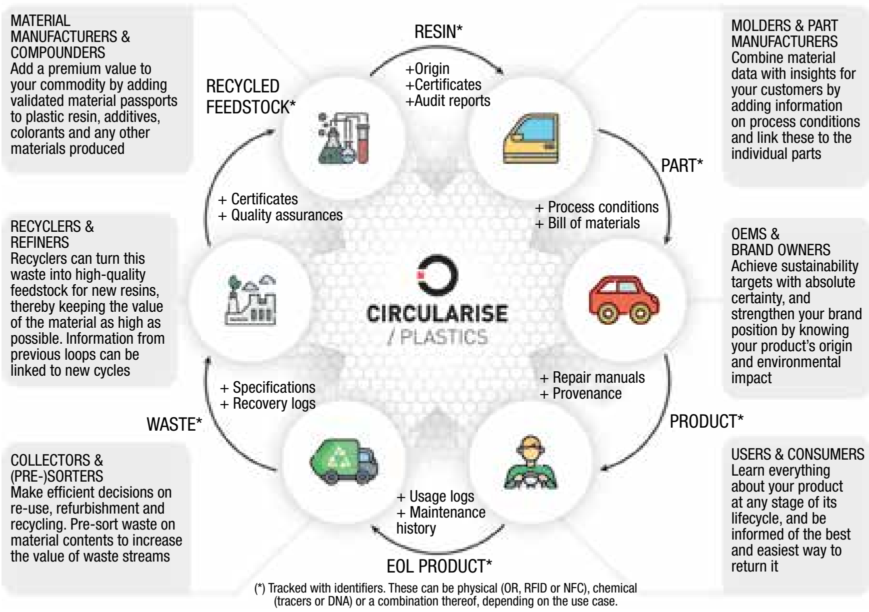


**FIGURE 1. Circularise Plastics is a comprehensive, blockchain-based platform aimed at improving supply-chain visibility for new resins, end-of-life (EOL) products, finished parts and more**

The Circularise platform (Figure 1) creates a digital twin of a material, component or product to build end-to-end traceability by integrating audit reports, certifications, material parameters and more. In addition to making materials traceable, Circularise aims to protect stakeholders' privacy — the protocol is specifically developed to enable the disclosure of relevant supply-chain information without having to share sensitive data. One facet of the Circularise Plastics program is the creation of "material passports," which contain all the verified information attached to a particular material, including batch number, certificates of analysis and more. "For example, when a material is being recycled, the recycler, and subsequently the customer, would know exactly where the material originates and exactly what it is made from," explains Burkhard Zimmermann, head of strategy, sustainability and digital at Covestro's Polycarbonates business unit.

The Circularise initiative aims to advance sustainability concepts — beyond just looking at plastics recyclability — and enable a communication protocol to facilitate their implementation. "This project can give us a sustainable feedstock of recycled plastics over time, yet also acknowledge additional benefits throughout the value chain and support customers in their search for sustainable materials," emphasizes Thomas Nuyts, global product director of Domo's Engineering Plastics segments.

Investment activities are further highlighting the economic importance of sustainable sourcing. In September, blockchain-based product-tracking platform OpenSC (Sydney, Australia;

www.opensc.org) — co-founded by the World Wide Fund for Nature and BCG Digital Ventures — received $4 million in seed funding to further develop its technology to trace, verify and share supply-chain data (Figure 2). OpenSC assigns a digital identity to a product and uses IoT technologies to trace its supply chain from origin to consumer. Collected data are stored in a decentralized, tamperproof blockchain. "The benefit of blockchain is twofold. Firstly, it's an immutable ledger, which means that once the data are recorded, it cannot be changed. The second benefit is that public blockchains are accessible and decentralized, so data can be made open and visible to consumers and other interested parties," explains Markus Mutz, CEO of OpenSC. OpenSC utilizes machine learning to synthesize meaningful insights and verify ethical production claims by processing large amounts of previously underutilized data from disparate sources — including satellite images, GPS information, weather patterns and more.

OpenSC recently announced a pilot project with global food manufacturer Nestlé S.A. (Vevey, Switzerland; www.nestle.com) to trace milk products from New Zealand to the Middle East, and plans are in place to expand this partnership to trace palm oil sourced in Mexico. Palm oil is a ubiquitous ingredient in numerous food and personal-care products, but its procurement is currently fraught with environmental risks related to deforestation, making it an area where innovative supply-chain strategies are necessary. "OpenSC can use technology to verify that a palm-oil product was farmed on deforestation-free land by analyzing satellite imagery over time. This can be overlaid with plantation boundary coordinates and a unique product identification, tracing the product back to a particular property, verifying that it was produced without deforestation," says Mutz. Palm oil is just one example of a product chain that can benefit from the data transparency provided by the customizable blockchain platform. Moving forward, Mutz believes that new levels of openness enabled by blockchain and other IoT technologies will drive consumers to increasingly demand sustainably sourced goods and encourage manufacturers to manage their supply chains to mitigate waste, fraud and other risks.

The need for responsible sourcing in the mining and minerals sector has been amplified by the tremendous growth in demand for battery materials, such as cobalt, graphite, lithium, lead, nickel and manganese. "The circumstances under which battery materials are produced, traded and transformed in certain geographies is fraught with risks," explains Nicholas Garrett, CEO of RCS Global Group (Berlin, Germany; www.rcsglobal.com). RCS Global has collaborated with IBM (Armonk, N.Y.; www.ibm.com) and a consortium of large-scale mining companies, automotive manufacturers and intermediate suppliers to develop the Responsible Sourcing Blockchain Network (RSBN), said to be the mining industry's first blockchain-based endeavor to tackle supply-chain sustainability. The RSBN includes an integrated assurance mechanism incorporating RSC Global's audits, which consider standards and guidance from the Organisation for Economic Cooperation and Development (OECD; Paris, France; www.oecd.org), including verification against human rights abuses. "For each tier of the supply chain, additional criteria can be applied, including, but not limited to, social, environmental or operational health and safety conditions," adds Garrett. The RSBN platform also aims to promote the socioeconomic advancement of small-scale miners through a tokenization model. Furthermore, the platform is designed so that it can be expanded to include additional conflict minerals and precious metals, with the goal of making it the industry standard for fully assured material traceability and provenance.

In addition to the RSBN, RCS has developed a smartphone application for data collection from remote mining sites. However, Garrett emphasizes, even with the abundant capabilities of digital technologies, a "boots on the ground" approach remains key in high-risk supply chains to ensure data integrity and for downstream companies to gain full visibility into their supply chain. "Our global supplier audit program helps clients map their entire raw-material-specific supplier ecosystem and verify that this ecosystem adheres to responsible sourcing practices, including industry policy frameworks, corporate codes of conduct and legislative requirements," adds Garrett.

OpenSC


**FIGURE 2.** OpenSC depends on blockchain technology to bring together data from disparate sources, creating a holistic view of a material's provenance

Another key element in assuaging supply-chain concerns is the collaborative management of relationships between suppliers and customers. "Enterprise contract management provides supply-chain visibility by tracking what a firm's worldwide obligation, entitlements and business relationships truly are. It gives a firm grasp on the supply chain, key suppliers, the composition of the products purchased and the locales in which they operate," says Neal Singh, chief operating officer at Icertis (Bellevue, Wash.; www.icertis.com). Icertis offers blockchain and artificial intelligence (AI) technologies to help companies improve transparency, execution speed and compliance with regard to measuring supplier diversity and product provenance. In the pharmaceutical sector, for instance, the complexities surrounding global supply chains, regulatory programs and drug trials introduce unique issues rooted in contract management and data visibility. "We're seeing more customers with the need to enforce regulatory compliance across multiple geographies and optimize their relationships with material suppliers," adds Singh.

## Innovations in materials use

The major drivers for responsible sourcing in the plastics supply chain are twofold — manufacturers must consider the sustainability of their raw materials while also minimizing the carbon footprint of producing plastic products. Dow (Midland, Mich.; www.dow.com) has advanced its sustainability strategy with technology partnerships focused on recycled and

Dow


**FIGURE 3.** Dow has received its first delivery of Fuenix renewable feedstock at its manufacturing site in Ternuezen, the Netherlands

renewable raw materials, as well as by making their products more readily recyclable. Dow has begun work with Fuenix Ecogy (Weert, the Netherlands; www.fuenix.com) based around feedstock recycling. Fuenix operates a plant that processes post-consumer wastes, such as multilayer films and food packaging, into a pyrolysis oil that Dow then uses in its crackers in place of traditional fossil-fuel feedstock for plastics manufacturing (Figure 3). A key benefit, points out Carsten Larsen, Dow's commercial director, Recycling EMEA & APAC, is that the "virgin" plastics produced using Fuenix recycled feedstock can be used in food-contact applications, whereas many other products that use recycled materials cannot, since the process using Fuenix feedstock is identical to typical plastics manufacturing. Through its partnership with Dow, Fuenix is working to scale up this technology. "This could be a very significant circular economy success story," says Larsen. Another partnership finds Dow producing plastics from a renewable naphtha fraction provided by UPM Biofuels (Helsinki, Finland; www.upmbiofuels.com). UPM produces its renewable naphtha from tall oil, a residue from pulp-and-paper processing. Like the Fuenix partnership, UPM pulp-based naphtha gives Dow a renewable source to make plastics that can then be deployed into higher-value products, including in food-contact applications. Using UPM feedstock, Dow has already produced thousands of tons of renewable polymers. Now, says Larsen, the company is looking to expand the use of these renewable polymers into new high-value application areas, including footwear. Larsen emphasizes the importance of using plastics only where they are the most sustainable choice of material. "We should be able to enjoy the benefits of plastics — decreasing food waste, safer transportation or sterile medical instruments — without the negative environmental impact. We must collaborate with waste-management and technology partners to make sure we can maintain plastic as a sustainable material."

Dow's renewable-plastics supply chain has been verified by the International Sustainability & Carbon Certification (ISCC; www.iscc-system.org), a rigorous auditing process that examines a product's entire lifecycle, from the raw material supplier to the production and post-processing facilities. "ISCC requires that you document and prove the amount of renewable feedstock or waste-plastic feedstock you bring into your operation and how much of that is turned into final product. It's quite a thorough certification process," says Larsen.

In the interest of making the supply chain for polyvinyl chloride (PVC) more sustainable, Perstorp AB (Perstorp, Sweden; www.perstorp.com) has become the first chemical manufacturer to gain certification from ISCC for renewable polyols, including the plasticizer Pevalen Pro. "The ISCC system has over 3,700 certificates in more than 100 countries. For Perstorp, reliability and transparency were essential when developing pro-environmental polyols, and we wanted to use a globally recognized third-party certification system," explains Anna Berggren, business development director at Perstorp. By employing bio-based alternatives to traditional raw materials, Perstorp makes Pevalen Pro in three different grades, ranging from 8 to 40% renewable content. "Pevalen is a pentaerythritol tetravalerate (PETV), which is formed by combining one pentaerythritol molecule with four valeric acid molecules. In the production of the raw material valeraldehyde, we can use biogas instead of natural gas; and for pentaerythritol, we can change acetaldehyde to bio-acetaldehyde and the methanol to bio-methanol," explains Jenny Klevås, Perstorp market segment manager, plasticizers. She points out that while it is not currently possible to make Pevalen Pro with 100% renewable content, it is the company's ambition to secure additional supply of renewable raw materials to make completely bio-based products. Beyond its renewable polyols, Perstorp has several other sustainability-focused projects in the works. "Besides our non-phthalate plasticizers, Perstorp is also developing new fertilizers that are based on formate chemistry, as well as a new polyester that can replace glass, styrene or polycarbonate in disposable and reusable packaging," mentions Perstorp innovation director Linda Zellner.

Another recent project aims to improve the supply chain for acrylic acid (AA), a commodity chemical used in numerous products, from diapers to paints. Nearly all AA is made from petroleum-based materials, but Archer Daniels Midland Co. (ADM; www.adm.com) and LG Chem (Seoul, South Korea; www.lgchem.com) are developing a technology to manufacture 100% bio-based AA using ingredients from corn processing. "We plan to leverage experience in feedstocks and process from both parties to advance the project to commercialization," says Paul Bloom, ADM's vice president for process and chemical research. At this point, portions of the technology have been demonstrated from laboratory- to full-scale operation. As part of the project, LG Chem is exploring the construction of a bio-based AA production plant in the U.S., and also evaluating additional opportunities in bio-plastics production. Bloom believes that the project is an excellent example of the type of cross-industry collaboration that is essential in advancing sustainable manufacturing processes. "Both parties bring unique processing experience. Between the companies, the team possesses the key capabilities to develop not only the technology, but the supply-chain integration needed to commercialize this new route," he adds. ■

*Mary Page Bailey*

# Improved Water Treatment Technologies Make Waves

## Greener chemistries and equipment advances provide more sustainable water-treatment options for chemical processors

### IN BRIEF

WATER REUSE

IMPROVED TECHNOLOGIES

GREENER CHEMISTRIES

COMBINED APPROACH

Chemical processors face tough challenges when it comes to the water used in the facility — namely, water scarcity and ever-increasing regulatory requirements associated with discharging effluent. At the same time, there is a move toward sustainability and "greener" approaches to all aspects of chemical processing, including water treatment. As these two forces collide, there is a growing trend toward water reuse and more environmentally friendly approaches to water treatment, which has resulted in not only new technologies and greener chemistries, but also novel combinations of these technologies, allowing processors to reuse water and treat both recycled and discharged water in a way that is easier on the environment.

"Earth has naturally recycled water for millions of years; however, pressure from scarcity, increased demand and the rising cost of treated water have influenced industries to review their method of consumption of water and treatment methods," says David Gilbert, director of engineering, with EMO3 (Quebec City, Canada; www.emo3.com). "In addition, pressure from federal and state regulators has motivated action to find enhanced methods that address effluent discharge water."

He continues: "Some of the primary goals of water reuse are to limit the use of available groundwater and aquifer for industrial processes, to decrease discharges to sensitive water ecosystems and increase groundwater recharge. The greatest challenge facing chemical processors is the huge cost of off-site disposal. This burden can cost up to $6 per gallon, depending on the contaminant and local discharge regulations, and the costs are increasing due to more stringent regulations. Hence, the interest and increasing adoption of onsite treatment systems."

### Water reuse

While water reuse is not a new practice, it is rapidly accelerating due to water scarcity issues, as well as the increasing costs of obtaining water for use in processes and treating water for discharge (Figure1). In addition, many companies are self-imposing sustainability practices involving water, says Kevin Milici, vice president of marketing and technology, with U.S. Water (St. Michael, Minn.; www.uswaterservices.com). "As a result, they see water reuse as an opportunity to help curtail the consumption of fresh water in a significant way and it is driving the practice."

U.S. Water

**FIGURE 1.** While water reuse is not a new practice, it is rapidly accelerating due to water scarcity issues, as well as the increasing costs of obtaining water for use in processes and treating water for discharge

Meeting the demands of minimal liquid discharge (MLD) and zero liquid discharge (ZLD) is another driving force behind reuse options. "Chemical and petrochemical facilities with large wastewater streams are increasingly looking to reduce or reuse liquid discharge. Though there has been significant progress, completely eliminating the gap between MLD and ZLD can be prohibitively expensive in terms of capital and operating costs," says Alexander Lane, commercial director, DuPont Water Solutions EMEA (Luzern, Switzerland; www.dupontwatersolutions.com). "At a 95% water recovery rate, a MLD approach can be operated at a fraction of the cost compared to a 100% ZLD system. By using cost-effective membranes, chemical processors can reduce the volume of water that needs additional dewatering via expensive thermal ZLD methods."

He continues: "Advancing a circular economy — in which raw materials are continually recycled and reused — is of increasing interest as brands seek to maximize the efficient use of water, close the resource loop and protect their license to operate. Sustainability is no longer a separate activity — it is inherent in the business plan."

Milici says recycled water is not just used for irrigation or flushing toilets in the facility (although it does have application here), but also for tasks directly related to operation. "We are seeing trends towards replacing fresh water with recycled water in ancillary systems like emission control to scrub waste gases and in applications such as steam generation and cooling water," he says.

Milici provides examples of how these applications might look in the facility. A plant may be using reverse osmosis (RO), a membrane-based technology, to produce high-purity water for the generation of steam (Figure 2). Raw water comes into the RO system, which produces clean process water. The reject, or brine, from that system would typically go to waste treatment. However, processors can now take that brine and, with adequate treatment chemistries, use it to become make-up or partial make-up water for applications such as cooling towers. "So now instead of using fresh water for the RO unit and the cooling tower, they are taking the waste stream from the RO unit and it becomes the primary source of, and replaces, fresh water for the cooling tower."

U.S. Water

DuPont Water Solutions

**FIGURE 2 (LEFT).** A plant may be using reverse osmosis (RO), a membrane-based technology as shown here, to produce high-purity water for the generation of steam
**FIGURE 3 (RIGHT).** Filmtec Fortilife RO elements are designed to tackle bio-fouling, organic fouling and scaling and can recover water from brine with salt levels ranging from 0 to 80,000 mg/L

EMO3


**FIGURE 4.** Taurus is a modular, ruggedized unit for highly efficient ozone treatment processes

Another application might be cooling tower blowdown recovery. You may have a cooling system with make-up water coming into it and bleeding off a continuous stream of water under controlled conditions. Again, instead of taking effluent from the cooling system and sending it to waste treatment, it can be reused right on the spot. "Different forms of filtration and membrane-based technologies can treat the wastewater from the cooling tower and bring it to the front end to use as a source of make-up [water] in lieu of brand new, fresh water."

In addition to the straight-up benefits of water reuse, this type of circular economy, according to Lane, considers "fit-for-purpose" water quality requirements versus strictly environmental discharge requirements. "The 'fit-for-purpose' water requirements are often more relaxed, meaning that water can be treated to the level needed for the intended purpose. For example, the concentrated reject stream from RO wastewater reuse systems can be a reliable water source for industrial plants and requires a varied level of treatment compared to water being reused for drinking. Additionally, when recycling and recovering pure water for circular water management, the trace contaminants in the water can be elevated, making them easier to capture and remove."

Fortunately, Lane says, product and technology innovation has improved many of the factors that go into water treatment, such as cost, energy, chemical use and maintenance. "Traditional processes like RO, ion exchange and filtration are gaining traction as more cost effective, sustainable methods for companies to improve their water footprint — enabling recovery of up to 95% of liquid discharges."

## Improved technologies

Often, traditionally applied wastewater recovery methods are not equipped to handle the challenges presented when water contaminants, including suspended solids, hardness, dissolved organics and high-salt levels are concentrated to extreme levels, but advances in proven technologies such as RO, ultrafiltration, nanofiltration and ion exchange used in a way that is tailored to each unique wastewater treatment challenge are making it possible.

For example, existing technologies such as RO, ultrafiltration, nanofiltration and ion exchange, are now being used in new ways for MLD, says Lane. "DuPont Water Solutions' Filmtec Fortilife RO Elements [Figure 3] help reduce costly concentrate waste, lower operating expenses and enable customers to move toward MLD," he says.

Bionetix

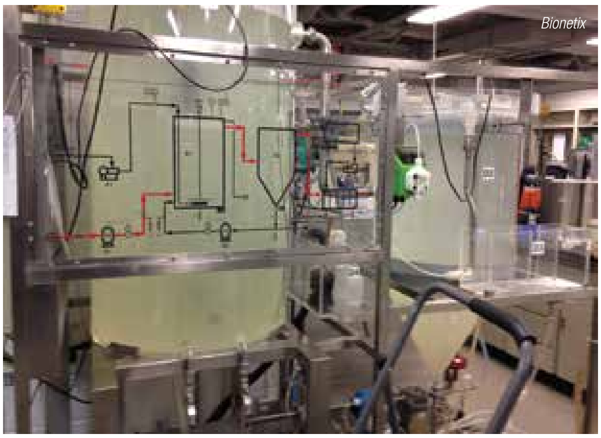

**FIGURE 5.** Bionetix natural wastewater solutions are specially targeted microorganisms and nutrients that degrade waste compounds such as grease, starch, petroleum hydrocarbons, cellulose, manure and ammonia

The company's Amberlite IRC83 Weak Acid Cation resin can be used in combination with RO to help facilitate higher productivity and lower operational costs. Additionally, DuPont's Tequatic Plus F-75 filters can be used as an alternative to bag filters. "We've seen the volume of recycled produced water reach levels close to 100% while reducing operating costs by about 60%," says Lane.

Another area of interest is in the use of ozone treatments, says EMO3's Gilbert. "Ozone technology is a mature one, but there has been an increasing interest in it following the detection of pharmaceutically active and endocrine-disrupting compounds (EDCs) in reclaimed water," he says. "As a sustainable technology, $O_3$ is produced onsite using compressed air or $O_2$. $O_3$ has the secondary benefits of not releasing toxic disinfection byproducts in the discharge."

Advances in electronic technology have recently permitted modular, higher frequency/higher voltage $O_3$ cells with a smaller footprint and lower cost to address a multitude of sustainable water oxidation/disinfection needs. "Our latest $O_3$ technology platform, Taurus [Figure 4], is a modular, ruggedized unit for highly efficient $O_3$ treatment processes. Every unit provides a constant concentration of 50 g/h of $O_3$," he says.

For applications that require removal of dissolved salts, a tunable water-deionization technology, known as capacitive deionization, or Cap DI, is making waves. "We're finding that it is favorable to use electrostatic attraction to remove dissolved salts from water," says L. Bryan Brister, CEO of Voltea (Farmers Brand, Texas; www.voltea.com). "The reason is that once salt dissolves into water, it dissolves into a molecule that carries a positive charge and, separately, a molecule that carries a negative charge, so the idea with electrification is very simple. Using direct current you can have a positively charged electrode surface and opposite that, a negatively charged electrode surface through which the water flows freely and the natural phenomenon of oppositely charged species attracting each other creates a scenario where positively charged salt is attracted to

the negatively charged electrode and the negative salt is attracted to the positively charge electrode.

He continues: "Over the last few years, Cap DI has become more practically possible. The reason is that while the material science that allows it to work had been very expensive, it has recently gotten to the point where the components are reliable, robust and inexpensive enough to make sense in the real world."

While Cap DI has many applications, in industry it is often used in wastewater reuse applications where it is installed after membrane bioreactor (MBR) and sequencing batch reactor (SBR) systems to enable customers to re-use the effluent for a variety of applications, such as cooling towers, boiler feed and irrigation. For these applications, Cap DI recovers up to 95% of the effluent with minimal chemical and power usage.

In cooling-tower applications, the water contains natural salts, such as calcium, bicarbonate, chloride and sulfate. The salts do not evaporate, so they build up over time, causing corrosion and scaling. To prevent this, chemicals are the traditional solution. However, CapDI can be used to treat the water before it enters the cooling tower, reducing salts from the incoming water stream by 80%. The cooling tower does not need to be adapted since CapDI is placed before it, treating only the incoming water, therefore the composition of the recirculating water remains unchanged. This increases the cycles of concentration significantly, resulting in lower overall water consumption and wastewater production.

## Greener chemistries

"Industry is trying to be more efficient and prudent in the use of chemistries in water treatment and, as result, they are selecting chemistries that meet environmental requirements and that means moving in a greener direction over time," says U.S. Water's Milici.

One such product comes from Bionetix International (Quebec, Canada; www.bionetix-international.com), which offers natural wastewater solutions in the form of specially targeted microorganisms and nutrients that degrade waste with greater efficiency. Bionetix offers products that target waste compounds such as grease, starch, petroleum hydrocarbons, cellulose, manure and ammonia (Figure 5). While these are often used at the wastewater-treatment facility, they can be used by chemical processors and other industries, as well.

According to Julie Holmquist, marketing content writer for Cortec Corp. (St. Paul, Minn.; www.corteccvi.com), the parent company of Bionetix, "A lot of wastewater treatment plants have limits on the level of BODs and CODs [biochemical oxygen demand and chemical oxygen demand] they will allow a chemical plant to release with their waste. If the facility has a BOD or COD measurement that is above this level, they can face fines due to the extra load of contaminants. But, if the chemical processor applies our products to their wastewater, they can cut down on the BOD and COD

SUEZ

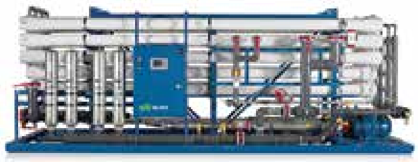

**FIGURE 6.** PRO Series Reverse Osmosis systems are well suited for a variety of applications and may be part of a treatment program that also includes greener chemistries

levels before they release them to the wastewater facility."

While using natural mechanisms for wastewater treatment is not uncommon, the microorganisms in Bionetix "have a certain appetite for different types of contaminants and are better at creating a certain type of enzyme," she says. "For example, if there's a starch factory, they would be creating a waste stream with extra starch in it, so the targeted organisms used in that application would produce the type of enzyme that breaks down starch. Bionetix takes microorganisms that are very good at degrading a certain type of contaminant and they target those based on what kind of waste the facility is producing."

One of the common regulatory issues from a discharge point of view is the use of phosphates in water-treatment applications, such as cooling towers. "Phosphates have been used for control of corrosion or formation of mineral scales and deposits in heat-transfer surfaces. But the problem with phosphates is that they eventually end up in a receiving body of water and those contaminants create problems in the environment," says U.S. Water's Milici. "So there has been a development of technologies that provide the same degree of corrosion protection as traditional phosphates but without the use of phosphates in the formulation. These 'Non-P' cooling-water treatments represent a very serious and significant advance in technology on the chemistry side of water treatment."

Peter Macios, executive product manager with SUEZ Water Technologies & Solutions (Trevose, Pa.; www.suezwatertechnologies.com) agrees: "Users of these chemistries are moving toward greener products that provide more of a filming protection around their assets and provide better protection without creating a foulant," he says. "Our latest offering is a program called E.C.O. Film, or Engineered Carboxylate Oxide, which is a technology that is designed to provide complete scale and corrosion protection in open cooling-water systems without the use any phosphorus or EPA [U.S. Environmental Protection Agency] priority pollutant materials. Our technology allows customers to go phosphorus-free and get the same performance and same corrosion protection at essentially the same cost to treat."

## Combined approach

Often, chemistries such as E.C.O. Film fit into a combined approach to water treatment. "If we think about a petrochemical plant, we are looking at how we allow them to use alternate water sources and typically the first stages of that is an equipment offering like membrane or ultrafiltration technology," he says. "And, if there's still contamination in that water, how do we use that water in the cooling water system without fouling? That's where greener chemistries and new filming technologies come into play," (Figure 6).

Milici from U.S. Water agrees: "Water treatment today is trending toward looking at each situation and providing a combination of chemistry, engineering, equipment and services that result in the optimal, best solution for a given application, and the solution is usually unique from plant to plant."

He continues: "What's really evolving, more than just the equipment or just the chemistry, is the combination of those technologies and how the different components are put together to solve particular problems with the smallest footprint and lowest capital costs possible." ■

*Joy LePree*

# Focus on Packaging

## Label applicator with enhanced IoT capabilities

The Herma 500 Label Applicator (photo) is an internet-of-things (IOT)-enabled machine utilizing realtime metrics to optimize production efficiency and consistency, even in a multi-factory setting. Capable of achieving labeling speeds up to 200 m/min, the Herma 500 can handle label widths between 80 and 320 mm and roll diameters from 300 to 600 mm. The Herma 500 is also exceptionally fast, with a maximum speed 70 ft/min higher than its predecessor. A maximum speed of 650 ft/min can be reached. — *Herma US Inc., Fairfield, N.J.*
**www.herma.us**

## Vacuum technology for dust-free filling of fine powders

With the Velovac vacuum technology, the bagging of fine powders (particle sizes smaller than 200 µm, bulk density of 10–450 g/L) takes place in a completely enclosed vacuum chamber. In this chamber, an atmospheric vacuum is generated through which the product is sucked into the vacuum bags. Any escaping dust is removed by suction and immediately redirected into the bagging process. In this way, none of the valuable product is lost. In addition, this process is particularly gentle on the product. Depending on the compaction potential of the material to be packed, a maximum product compaction of up to 400% is achieved, says the company. — *Greif-Velox, Lübeck, Germany*
**www.greif-velox.com**

## This stacker features powered lift and drive

The PowerStak family of high-performance, fully powered stackers (photo) offer significant performance advantages over manual stackers and significant cost savings versus forklift trucks, says the company. Because PowerStak features both powered lift and powered drive, operation is nearly effortless for any operator regardless of their size or physical strength. Compact design, low overall weight, and quiet operation allow them to fit into a wide variety of work environments, including warehouses, loading docks, manufacturing and assembly work cells, retail and more. All models feature an ergonomically designed control handle that puts all functions, including lift, lower, forward and reverse, within easy reach. Redundant design allows all controls to be accessed by the operator's right or left hand. PowerStak Stackers are available in multiple configurations, handling capacities from 1,000 to 3,000 lb and lifting heights of up to 150 in. — *Presto Ecoa Lifts, Norton, Mass.*
**www.prestolifts.com**

## These load stops ensure perfect pallet placement

This manufacturer of material-handling products recently introduced its new bolted Pallet Load Stop Option (photo). Designed for heavy-use applications, the Pallet Load Stop provides an added layer of protection for personnel safety and inventory loss. The pallet stoppers allow perfect placement of pallets – providing a fixed 6-in. flue space for pallet rack applications. The pallet safety stops allow for ventilation and provide space for fire-suppression sprinklers above the racks to penetrate product stored in racks. The new bolt-together pallet-load-stop design provides users with the flexibility of either a 3- or 4-in. set back using the same clip. Bay widths of 96, 108 and 144 in. are stock items. — *Steel King Industries, Inc., Stevens Point, Wis.*
**www.steelking.com**

## This packaging-line lift has an integrated scale and conveyor

Integrating the height adjustment of a scissor lift with digital weighing and conveying functions makes the Scissor Lift Table (photo, p. 22) an optimal solution for a packaging line filling station. The system has lifting capacities of 2,000–6,000 lb. Manual turntables can also be added for improved operator ergonomics and product po-

*Herma US*

*Presto Ecoa Lifts*

*Steel King Industries*

Note: For more information, circle the 3-digit number on p. 58, or use the website designation.

Verti-Lift

Sterling Systems & Controls

The L.S. Starrett Co.

Schütz

Marchesini Group

sitioning. A variety of conveyor tops are available. Optional accessories include accordion skirts, oversized platforms, platforms with beveled edges, pit-mounted, portability package, PLC control, foot-pedal control, high-cycle and external power units. The lifts are also available in pneumatic designs. — *Verti-Lift, Inc., Louisville, Ky.*
**www.verti-lift.com**

## A system for packaging and unloading bulk bags and more

The new Bulk Bag Packaging Systems (photo) can fit a wide range of bag and container sizes and can handle filled capacities from 100 to 4,400 lb. The Bulk Bag Packaging Systems include an adjustable upper frame to accommodate square and rectangular containers. Heavy-duty weighing controls are built to withstand the rigors of industrial use. Easy loading and bag discharging is accommodated with bag loop holders. Inflatable fill heads assure dust-tight filling, even with fine powder materials. The system can also accommodate drums and totes, and can be customized to include a wide range of options for automatic and manual filling applications. — *Sterling Systems & Controls, Inc., Sterling, Ill.*
**www.sterlingcontrols.com**

## Video-based measurement system offers increased speed

The new generation of HDV300 and HDV400 bench-top Digital Video Comparators (photo) boast a number of enhancements. CNC (computer numerical control) motion on the new HDV systems is said to be significantly faster than predecessors, enabling even greater user measurement throughput. At 10 mm/s, speed on the *Y*-axis has tripled, and *X*-axis speed has almost doubled at 45 mm/s. In addition, improved LED ring lighting provides a more consistent illumination. The computer and M3 controller in the new systems are located inside the HDV housing, resulting in a clean design with minimal external wiring and connections. — *The L.S. Starrett Co., Athol, Mass.*
**www.starrett.com**

## Maximum protection for demanding filling products

Intermediate bulk containers (IBCs) and drums from this company's Foodcert and Cleancert lines ensure comprehensive material, product and process safety. The company is now offering these IBCs with a liner system (photo) with U.N. approval, thus ensuring maximum quality protection with minimum effort. The Ecobulk Foodcert + Aseptic fully meets the specific requirements in the food, pharmaceuticals and toiletries industries; it effectively excludes contamination risks along the entire supply chain, extends the shelf-life of the filling products and ensures consistent quality from filling to emptying, says the company. The liner is made of top-grade LDPE (low-density polyethylene) film; a special folding technique minimizes air and allows it to unfold and align itself automatically in the inner bottle during filling. The gradual unfolding of the liner also means that contact between the filling product and the ambient atmosphere is kept to a minimum. The result is 99% less exposure to oxygen than in a standard IBC, says the company. — *Schütz GmbH & Co. KGaA, Selters, Germany*
**www.schuetz.net**

## Inspection technology keeps filling under control

Together with its partner SEA Vision, this company recently introduced the SV (photo), a semi-automatic machine for the inspection of liquid, lyophilized or powder products in ampoules, vials and cartridges or pre-filled syringes. The SV is equipped with brushless motors for fast rotation (before inspection) and slow rotation (during inspection) to guarantee complete and efficient product control. The containers are conveyed to the inspection station where the operator inspects them through a magnifying lens. The rejected products are automatically collected in trays. The machine can operate in line with other units or factory-set to be loaded and unloaded in trays with customized dimensions. It can be configured as multiple inspection stations placed sequentially or in parallel according to user requirements. Capacity ranges from 1 to 1,000 mL. The machine can handle up to 100 pieces per minute. — *Marchesini Group S.p.A., Bologna, Italy*
**www.marchesini.com** ■

*Gerald Ondrey*

# New Products

## This monitoring platform has built-in cybersecurity

The Orbit 60 Series (photo) is a next-generation condition-monitoring and protection platform that collects and processes data to evaluate machine health. It is said to be the first intrinsically cyber-secure machinery-monitoring platform with a built-in data diode, which enables secure one-way data transfer from the device to this company's System 1 machinery-management software for proactive monitoring and diagnostics. This platform offers 80 dynamic data channels, compared to the industry average of 50, with 1,200 times higher signal-processing power in a small physical footprint, says the manufacturer. The Orbit 60 system is certified to safety integrity levels (SIL) 2 and 3, and is compliant with API 670 standards. — *Bently Nevada, LLC, a business of Baker Hughes, a GE Company, Minden, Nev.*

**www.bently.com/orbit60**

## New flow and energy meters for non-invasive measurements

The Dynasonics TFX-5000 ultrasonic clamp-on flow and energy meters (photo) are designed for non-invasive, ultrasonic transit-time measurement for use in water and wastewater treatment, heating, ventilation and air conditioning (HVAC) and oil-and-gas applications. TFX-5000 meters measure volumetric flow and heating or cooling rates in clean liquids, as well as those with small amounts of suspended solids or aeration, such as surface water or raw sewage. By clamping onto the outside of pipes, ultrasonic devices like the TFX-5000 meter do not contact the internal liquid and have inherent advantages, such as reduced installation time and cost. The TFX-5000 devices are available in two versions: a flowmeter for water delivery, raw sewage, cooling water, sea water, deionized water, water-glycol mixtures, alcohols, chemicals and many caustic fluids; and a heating/cooling energy flowmeter used in conjunction with dual clamp-on resistance temperature detectors (RTDs) for temperature measurement in hydronic processes and HVAC systems. — *Badger Meter, Inc., Milwaukee, Wis.*

**www.badgermeter.com**

## Turbo blowers added to this company's product portfolio

This company has added PillAerator turbo blowers (photo) to its line of rotary-lobe and rotary-screw blowers. This action significantly expands offerings for the water and wastewater market and other large-flow, low-pressure applications, including bioreactors and fluegas desulfurization. Available with flowrates from 4,700 up to 10,000 ft$^3$/min, PillAerator blowers feature gas-tight, permanent magnet motors with active magnetic bearings, integrated frequency converters and closed-loop water cooling. Units are compact and quiet, and advanced controls offer full interoperability with SCADA systems. — *Kaeser Compressors, Inc., Fredericksburg, Va.*

**www.us.kaeser.com**

## These new drives feature enhanced safety functionality

The new Sinamics G120X drive (photo) is designed for use with pumps, fans and compressors in many industrial sectors, such as water, wastewater, HVAC, irrigation, agriculture and more. Sinamics G120X has a power range of 1 to 700 hp (0.75–630 kW) and can operate in a temperature range from –4 to 140°F with any standard motor, including synchronous reluctance motors (SRM). Sinamics G120X meets all the latest and upcoming UL, NEMA and EN/IEC standards and offers up to 100 kA short-circuit current rating (SCCR), ensuring enhanced product safety and energy efficiency, says the manufacturer. The compact design of the G120X saves space in the control cabinet, and it has hardware-based built-in safety functions that are certified to SIL 3. — *Siemens Digital Industries, Nuremberg, Germany*

**www.siemens.com**

## New membrane elements tackle biofouling in desalination units

This company has released the fouling-resistant seawater Filmtec SW30XFR 400/34 membrane element for reverse-osmosis systems. This new element has been specifically designed to address biofouling in seawater reverse-osmosis (SWRO)

Bently Nevada

Badger Meter


Kaeser Compressors

Siemens Digital Industries

Honeywell

Emerson


Hiden Isochema

desalination plants. Biofouling can cause serious operational problems by significantly reducing membrane life. The new Filmtec SW30XFR elements feature a fouling-resistant, low-pressure-drop design, along with a durable membrane chemistry. Industrial trials of the new SWRO elements showed a 40% lower pressure drop than previous product generations, with stable performance in terms of normalized permeate flow and salt rejection. Also, the new elements show promising chemical resistance, even in applications where clean-in-place processes occur frequently. — *Dupont Water Solutions, Wilmington, Del.*
**www.dupont.com/water**

## New software platform scales industrial cybersecurity

The Forge Cybersecurity Platform (photo) improves cybersecurity performance at a single site or across an enterprise by increasing visibility of vulnerabilities and threats, mitigating risks and improving management efficiency. The new platform safely moves data from one site to another and uses operations data to strengthen endpoint and network security, while improving cybersecurity compliance. Furthermore, users that may not have the cybersecurity expertise or resources to support the Forge Cybersecurity Platform can maximize their cybersecurity investment by utilizing this company's Managed Security Services to host and run the software — *Honeywell, Charlotte, N.C.*
**www.honeywell.com**

## New monitoring edge device accelerates asset digitalization

The AMS Asset Monitor edge analytics device (photo) digitizes data and analytics, with focus on essential assets that were previously monitored only with infrequent assessments. The new device connects with the Plantweb Optics asset-performance platform to provide instant asset-health details. Plants typically monitor the condition of essential assets such as pumps, fans and heat exchangers only every 30 to 60 days, but shortening this gap is essential to avoiding unexpected downtime. The new AMS Asset Monitor combines embedded logic-based analytics and intuitive health scoring to make it easier to monitor and maintain essential assets. The platform can help plan maintenance during scheduled shutdowns and turnarounds and reduce or eliminate unplanned downtime. Unlike typical analytics devices that send data to a historian or to the cloud to be processed later, AMS Asset Monitor provides analytics at the edge, performing calculations at the device level, reducing complexity and expense. Each device collects data continuously and uses embedded logic to identify and diagnose common reliability issues, such as imbalance, misalignment, bearing faults, lubrication issues or fouling, which are consolidated into an overall asset-health score. — *Emerson, St. Louis, Mo.*
**www.emerson.com**

## New analyzers measure binary gas sorption

The IGA-003-MC (photo) is a turnkey system for binary gas sorption that features a gravimetric analyzer, coupled mass spectrometer and an optimized gas-delivery and sampling system. Measuring multicomponent gas sorption equilibria is essential to characterize and assess adsorbents for many applications, such as nitrogen and oxygen production from air, natural gas upgrading and hydrogen purification. According to the manufacturer, IGA-003-MC analyzers provide faster measurements than traditional multicomponent sorption methods while requiring a much smaller sample size — usually just a few grams of material. The IGA-003-MC uses the recently developed Integral Mass Balance (IMB) sorption-analysis technique, which is unique to the IGA-003-MC product line. In the IMB method, a controlled gas mixture flows over a sample suspended from the IGA microbalance, and the gas composition at the outlet is determined using a mass spectrometer. Inlet flowrates and outlet gas composition are then combined with in-situ gravimetric data to calculate the partial uptake of each gas, as well as the total mass uptake, as a function of gas composition. — *Hiden Isochema Ltd., Warrington, U.K.*
**www.hidenisochema.com** ■

*Mary Page Bailey*

# Pneumatic Conveying: Pipeline Bend Challenges

*Department Editor: Scott Jenkins*

Among the key benefits offered by pneumatically conveying bulk solids is the ability to route materials around obstructions in the plant using bends in the pipeline. However, these changes in direction involve a considerable number of particle impacts on the bend wall as the particles make the turns. This one-page reference reviews the potential problems that can arise from particle impacts in pipe bends of dilute-phase pneumatic-conveying systems.

## Bend geometry

Pipe bends can take a variety of different geometries, which can have a significant influence on particle impact angle. Basic long-radius bends are the most commonly used because they provide the most gradual change in direction for solids, and because the angle of impact on the pipe wall is relatively small, which helps to minimize the risk of attrition or erosion.

Common-radius bends are made by bending standard tubes or pipes (Figure). The radius of curvature, $R_B$, may range from 1 to 24 times the tube diameter, $D$. Common-radius bends can be loosely classified as follows: Elbow ($R_B/D$ = 1 to 2.5); Short radius $R_B/D$ = 3 to 7; Long-radius ($R_B/D$ = 8 to 14; Long sweep ($R_B/D$ = 15 to 24).

## Pressure drop related to bend

As particle impacts occur, particularly against bends, there will be a significant reduction in particle velocity. These particles will then have to be re-accelerated back to their terminal velocity, which will add significantly to the pressure drop — and hence, energy loss — for the conveying system. This is particularly true after short-radius bends.

The pressure drop in a bend depends on the ratio of bend radius to pipe diameter, the gas velocity, $U_g$, and the internal roughness, $k$, of the pipe. When a two-phase, gas-solid suspension undergoes a directional change in a pipeline, the bend naturally acts as a segregator of the two phases. Centrifugal forces act on the particles, concentrating them near the outer wall of the bend. Friction coefficients within the bend will be different than those in the adjacent straight sections.

## Abrasion of pipe wall

If the material to be conveyed is potentially abrasive, significant wear of the pipeline, especially at the bends, is likely to occur. With a new bend, the particles tend to travel straight on from the preceding straight pipeline until they impact against the bend wall. After impact, they tend to be swept around the outside surface of the bend. They are then gradually entrained in the air in the following straight length of pipeline.

## Attrition of particles

If the material being conveyed is potentially friable, damage to the material being conveyed may occur, and it is possible that these changes to the material could affect the conveying performance of the material itself.

***Particle breakage.*** Particle breakdown occurs by three main mechanisms. The first is to shatter or degrade when the bulk solid is subject to impact or compressive loading. The second is for fines and small pieces to be worn away by attrition when bulk solids either rub against each other or against some surface, such as a pipeline wall or bend. The third is for the materials, such as nylons and polymers, to form "angel hairs" when conveyed, as a result of micro-melting, which occurs to due to the frictional heat of particles sliding against pipeline walls.

***Operating problems.*** Particle degradation can cause problems in a number of areas because of changes in particle shape and particle-size distribution that can result. Plant operating difficulties are often experienced because of the fines produced, and problems in handling operations can also result after the material has been conveyed. Apart from the obvious problems of quality control with friable materials, changes in particle shape can also lead to subsequent process difficulties with certain materials. The appearance of the material may also change, making it out of specification.

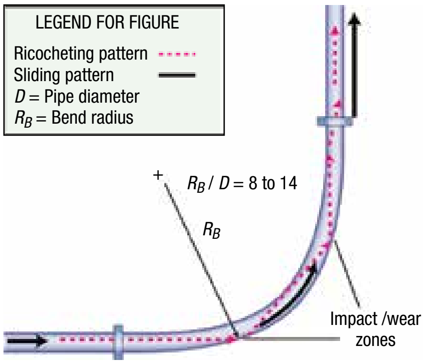


**FIGURE.** Flow in a standard, long-radius bend is illustrated here, with typical flow patterns, wear points and reacceleration zone shown

***Filtration problems.*** In pneumatic conveying systems, plant-operating difficulties can result if degradation causes a large percentage of fines to be produced, particularly if the filtration equipment is not capable of handling the fines satisfactorily. Filter cloths and screens will rapidly block if they have to cope with unexpectedly high flowrates of fine powder. The net result is that there is usually an increase in pressure drop across the filter, and this could be a significant proportion of the total pressure available in a low-pressure system.

***Flow problems.*** In many systems, there is a need to store the conveyed material in a hopper or silo. Flow functions can be determined for bulk particulate materials, from which hopper wall angles and opening sizes can be evaluated, to ensure that the material flows reliably at the rate required. A change in particle-size distribution of a material, as a result of conveying operations, however, can result in a significant change in flow properties. Thus, a hopper designed for a material in the "as-received" condition may be totally unsuitable for the material after it has been conveyed. As a result, it may be necessary to fit an expensive flow aid to the hopper to solve the problem. ■

***Editor's note***: This "Facts at your Fingertips" column is based on infomration from the following articles: Dhodapkar, S., Solt, P. and Klinzing, G., Understanding Pipe Bends in Pneumatic Conveying Systems, *Chem. Eng.*, April 2009, pp. 53–60; and Mills, D., Particle Impact Problems in Pneumatic Conveying, *Chem. Eng.*, March 2017, pp. 69–76.

# Nitrile Rubber Production

*By Intratec Solutions*

Nitrile rubber (NBR), also known as Buna-N, is a synthetic rubber copolymer of 1,3-butadiene and acrylonitrile. The material is resistant to various oils, fuels and chemicals, and is classified as a specialty rubber. NBR is primarily used in applications where good oil resistance is required, such as in rubber seals and O-rings, hose and belting stock, blowout preventers or packers (oil drilling). NBR is also used in molding miscellaneous parts, rubber latex products, sponge applications and footwear.

## The process

The process examined here is a typical continuous cold-emulsion process for producing NBR that contains 33 wt.% of acrylonitrile. The process (Figure 1) consists of three major sections: (1) polymerization, (2) purification and (3) finishing.

***Polymerization.*** Acrylonitrile and butadiene are mixed with an emulsifier agent, demineralized water and other chemicals to form the emulsion that will be fed to the polymerization reactors. Polymerization is conducted in continuously stirred, jacketed-tank reactors connected in series. To keep the reaction temperature low, all reactors are cooled by means of ammonia vaporization. Downstream, a shortstop agent is mixed with the emulsion in order to stop the reaction at the desired conversion level (75–80%). This action avoids gel formation.

***Purification.*** The latex generated in polymerization reactors is flashed at atmospheric pressure and then under vacuum. Residual butadiene vapors are compressed and then cooled for condensation. The condensed stream is directed to a decanter for water removal. Recovered butadiene is recycled to a butadiene plant, where butenes are separated, so the recovered butadiene can be reused in the NBR plant. The degassed latex is pumped and fed to a vacuum plate column, where residual acrylonitrile monomer is stripped by contacting the latex with steam that enters from the column bottom. Stripped acrylonitrile is condensed and then sent to the polymerization stage. The latex is transferred to the coagulation step.

***Finishing.*** Subsequently, the latex is mixed with an antioxidant, then mixed with brine and sent to a coagulation tank, where dilute sulfuric acid is added. The pH change of the latex from alkaline to acidic converts the soap into organic acid and the latex immediately coagulates and becomes small crumbs suspended in water. The resulting crumb material is washed with water, neutralized with caustic soda and dried in continuous-belt dryers that are heated by steam pipes. After drying, the rubber is pressed into bales, weighed, film-wrapped and boxed for sale.

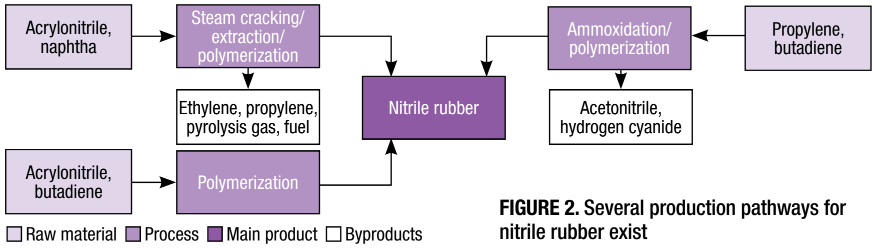


**FIGURE 2.** Several production pathways for nitrile rubber exist

## Production pathways

Nitrile rubber production involves the emulsion polymerization of 1,3-butadiene and acrylonitrile, so different NBR manufacturing routes are related to different sources of the monomers used. The most typical NBR production routes are based on acrylonitrile produced via ammoxidation of propylene and butadiene produced via isolation from C4 steam-cracker fractions. Different pathways for NBR production are presented in Figure 2.

## Economic performance

The total operating cost (raw materials, utilities, fixed costs and depreciation costs) estimated to produce NBR was about $1,950 per ton of nitrile rubber in the fourth quarter of 2015. The analysis was based on a plant constructed in the U.S. with capacity to produce 50,000 metric ton per year of NBR.

This column is based on "Nitrile Rubber Production – Cost Analysis," a report published by Intratec. It can be found at: www.intratec.us/analysis/nitrile-rubber-production-cost. ■

*Edited by Scott Jenkins*

***Editor's note:*** The content for this column is supplied by Intratec Solutions LLC (Houston; www.intratec.us) and edited by *Chemical Engineering*. The analyses and models presented are prepared on the basis of publicly available and non-confidential information. The content represents the opinions of Intratec only. More information about the methodology for preparing analysis can be found, along with terms of use, at www.intratec.us/che.

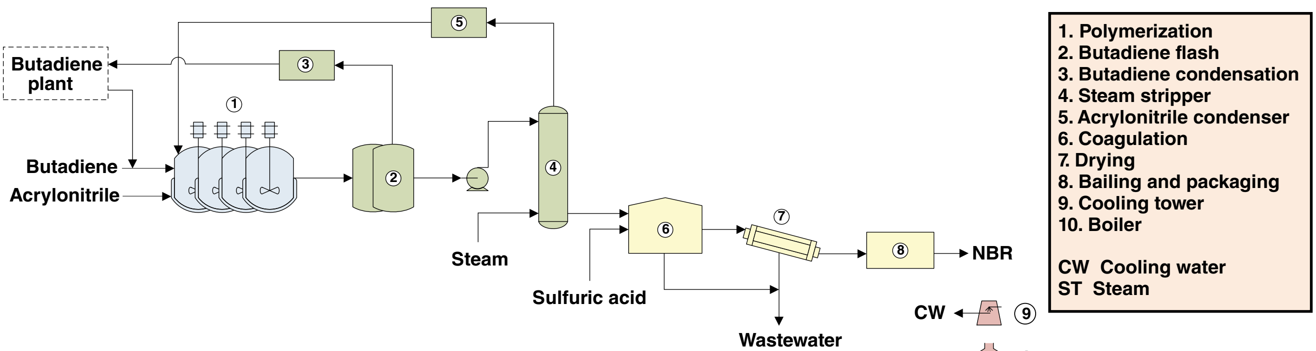


**FIGURE 1.** The diagram shows nitrile rubber production via emulsion polymerization

Part 1

# CFD: Driving Engineering Productivity

This article provides an overview of how computational fluid dynamics (CFD) works, and what benefits it can bring to the chemical process industries

**Hossam Metwally**
Ansys Inc.

## IN BRIEF

CFD DEFINED

EXECUTING CFD SIMULATIONS

HIGH-PERFORMANCE COMPUTING

ADVANCED CFD SOFTWARE

Sustainability, waste reduction, energy efficiency and increased demand for engineered material are driving process engineers to continuously investigate new products and processes, and develop ways to improve process and equipment safety, efficiency and reliability.

To accomplish this, engineers can leverage advanced product-development modeling tools, such as computational fluid dynamics (CFD), to conduct simulations that replicate the near real-life operating conditions of a plant or mimic product performance requirements. This virtual testing requires just a fraction of the time and cost of laboratory-scale or pilot-plant testing. It also reduces the need for expensive prototypes, delivers improved product quality and helps speed products to market.

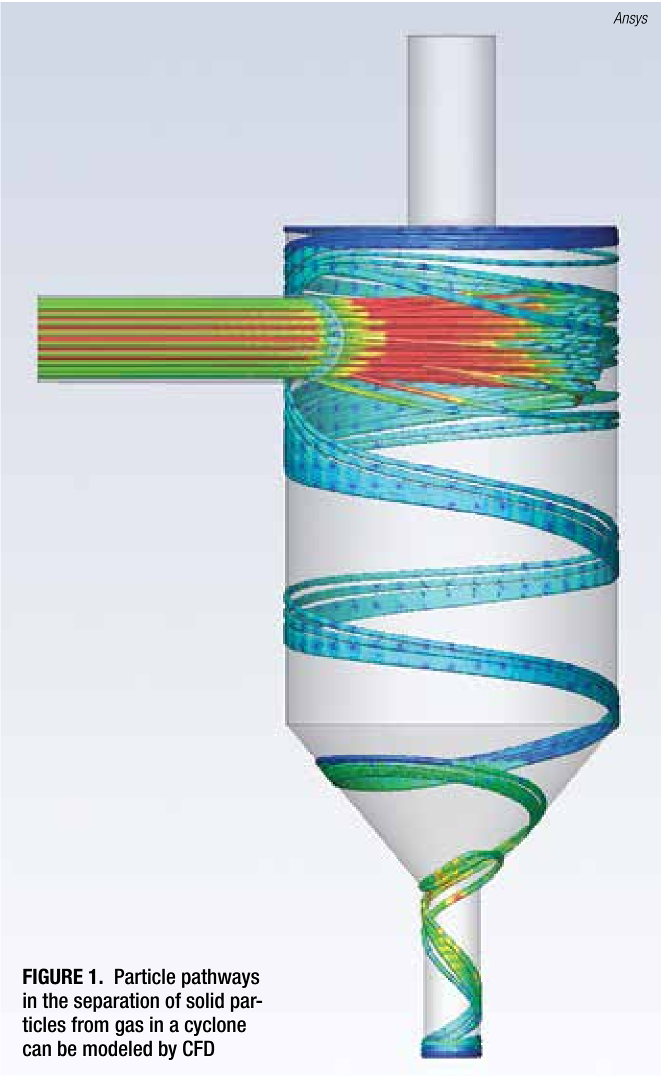


**FIGURE 1.** Particle pathways in the separation of solid particles from gas in a cyclone can be modeled by CFD

## CFD defined

Process engineers are familiar with plant design software and general mathematical modeling tools for process optimization. CFD is a branch of engineering simulation that solves the physics of fluids with or without heat transfer, mass transfer and chemical reactions, and is used for the design and analysis of equipment and unit processes. The idea is to predict, and design around, transport-related problems using detailed numerical-solution methods prior to physical testing. Alternatively, CFD simulations can provide operational support for troubleshooting, throughput improvement, process scaleup (and scaledown), and improving product quality and plant yield. The simulation can be

steady or dynamic – 2D or 3D – and subjected to initial, boundary and flow operating conditions.

The use cases for which CFD can be applied are unlimited, but examples of unit processes include separation (Figure 1), mixing (Figure 2), heat-transfer systems, flow measurement and control, and reactors of all types, including packed-bed and fluidized-bed reactors. The CFD simulation results can be used to optimize the product at concept development, product design inception or for equipment already deployed in the field. The key element of successfully applying CFD is the ability of CFD algorithms to allow the simulation of complex physical flow phenomena within complex machinery under realistic process conditions accurately and reliably.

CFD offers major advantages for the design and analysis process. Visualizing complicated flow features inside equipment can be quite complex. CFD enables engineers to create and explore "what if" simulated scenarios, providing them with detailed and comprehensive insights on flow fields, allowing them to virtually look inside their equipment. This enables the analysis, optimization and verification of design performance before building costly prototypes or undergoing time-consuming trial-and-error physical testing.

Simple CFD problems can be solved on laptops (for more information on CFD models using laptops, see Part 2 of this feature, pp. 33–39). More sophisticated problems — in terms of physics or problems size — may require high-performance computing (HPC) that offer large clusters with countless cores and terabytes of memory, delivering dramatically reduced turnaround times for complex simulations.

## Executing CFD simulations

Executing a successful CFD simulation that delivers meaningful end results requires considerable understanding of the problem being investigated. This typically involves the physics of fluid flow, mixing, chemical reaction and heat transfer. To achieve this, engineers must solve a set of mathematical equations that represent the problem of interest. CFD remains key for selecting and solving the physics-based equations "numerically," since these equations are essentially impossible to solve analytically. CFD's numerical or computational methods convert these equations into clear, linear algebraic equations and solves them numerically. Every CFD problem has the same general workflow, divided into four basic phases: model objective and domain extent, pre-processing, solving and post-processing.

***Model objective and domain extent.*** Before initiating a CFD model, a clear description of the problem must be developed. What exactly needs to be modeled? What are the quantities of interest that should be obtained from the model (for

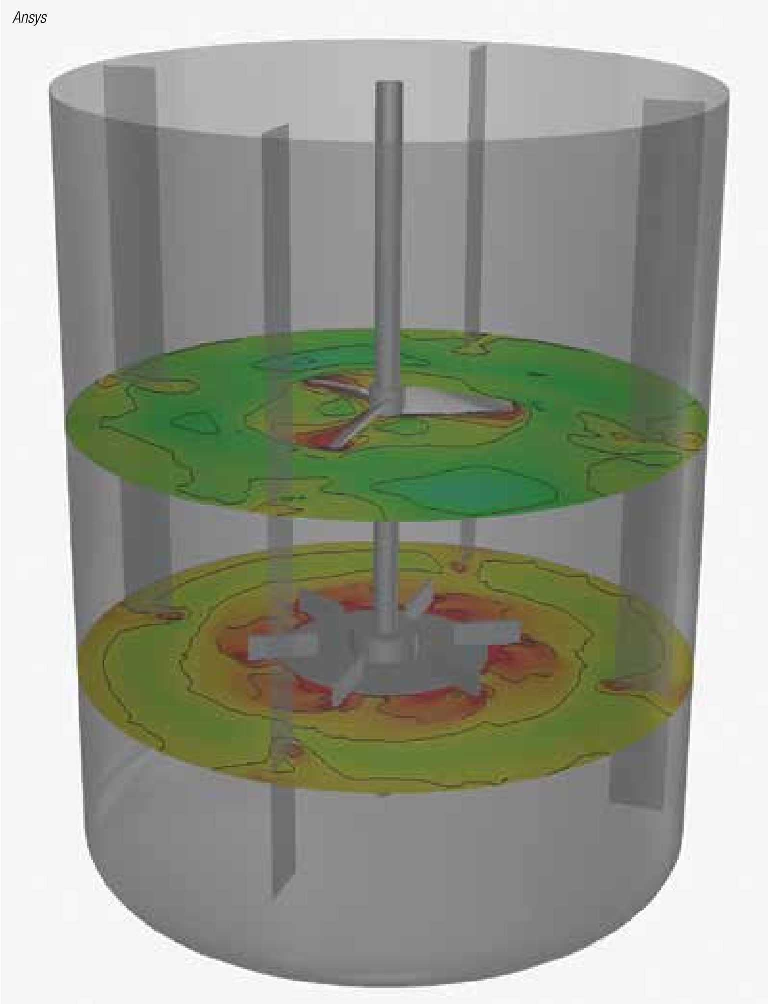


**FIGURE 2.** Shear rate variations in two planes passing through the impellers of a mixer can be shown with CFD

example, pressure drop, flow distribution, concentration of various materials, and so on)? Then comes the question of what the domain extent for that CFD model should be (for instance, a mixing tank or a heat exchanger). The next step is to discern whether all the process (boundary) conditions are known (such as inlet conditions and heating/cooling controls). Another important ingredient in CFD modeling is the definition of material properties for the various ingredients. Finally, the CFD model must be made as efficient as possible by figuring out what simplifying assumptions can be made, in terms of physics, process conditions and even geometry.

Answering these questions in CFD modeling provides "rigor" to the engineering process, which by itself helps with the definition, documentation, repeatability and scalability of the process.

***Pre-processing.*** During pre-processing, the first step is to prepare a geometrical computer-assisted design (CAD) model for CFD modeling purposes. The idea is to have a CAD representation that only contains the relevant geometrical features that will impact flow. Any unnecessary details or features should be omitted at this point.

Next, the discretization (mesh generation) of the flow domain plays a crucial role in the CFD workflow. While this used to be the most labor-intensive and time-consuming part of simulation, recent advances have streamlined this step tremendously. During discretization, CFD divides the CAD model into a finite number of discrete, small, individual regions called cells. This is analogous to a digital photograph where millions of pixels compose a single complex image, with each pixel possessing its own unique color. Analysts must strive for the optimal mesh that will capture flow features of interest, while keeping the overall model size in check.

To calculate the numerical solution in these individual cells, CFD computes all the flow variables (such as pressure and velocity) at the center (or node) of each cell, based on the values of velocity and pressure of its surrounding nodes. A large number of cells increases the solution's accuracy, but also increases the number of equations that must be solved.

***Solving.*** After discretization, the model can be set up for simulation. The set-up process involves the definition of the following:

- Boundary (or process) conditions, such as inlet flowrates, temperature and impeller speed (revolutions per minute)
- Physics, including laminar versus turbulent flow, steady versus unsteady, and so on
- Material properties, such as density, viscosity, thermal conductivity and specific heat

After the solver and physics model are established, the flow field can be solved. During the computing process, the solution must be monitored as modeling iterations are executed. This helps to understand the accuracy of the physical models, discretization and problem setup.

***Post-processing.*** Post-processing is the last step in the CFD workflow. In this step, the obtained results are visualized, analyzed and interpreted. CFD provides both quantitative and qualitative insights. Examples of quantitative results include flow, concentration and temperature contours across the domain. On the other hand, examples of qualitative results include information like the average temperature exiting the system or the total pressure drop experienced. Based on the results, the appropriateness of the selected discretization resolution and the physical model is measured and revisited as necessary.

## CFD for improving operations

CFD enables engineers to maximize throughput, innovate on new products, enhance process stability across the plant, drive sustainability and develop new processes more efficiently. The following are examples of how CFD can be applied to improve each of these.

***Flow distribution.*** Most chemical companies do not design their own plant equipment; rather, they own assets and operate them. The key issue is throughput and finding new ways to push more material through production. Can they get more from their assets than they already have? How can they manage flow distribution to avoid erosion, corrosion and extra pressure drops? How will existing assets behave under different products or materials?

CFD delivers both a virtual visualization of the flow, as well as a quantitative description of how uniform or non-uniform the flow will behave across any section of the system (Figure 3). Empowered with this predictive modeling, engineers can best determine how to ensure flow uniformity throughout the entire system to better maximize throughput, yield and the operational efficiency of plant equipment.

***Scaleup.*** CFD is also instrumental for supporting the scaleup process, especially in the chemical and pharmaceutical industries. During this process, engineers run experiments inside a laboratory on a much smaller piece of equipment to be tested. This bench- or laboratory-scale equipment is used to develop the product. Then, through the scaleup process, questions of how this product can be manufactured on the commercial scale are answered. CFD is used to estimate how the commercial-scale process will perform and the corresponding outcome on the product.

***Process stability.*** CFD also helps drive process stability. Chemical engineers must manage problematic issues, such as rust buildup in pipelines and fouling, erosion, hotspots, dead spots and cold spots in chemical plants. Through CFD modeling, engineers can predict and identify these issues before they materialize in the plant and deal with them to deliver an enhanced level of efficiency, reduce downtime and help ensure safety. Also, the stability of the process against process or material variability can be simulated using CFD.

***Process intensification.*** While engineers want production to run cheaper, better and more reliably, they also are focused on process intensification that allows greater energy efficiency and the creation of more sustainable products through reuse or product redesigns.

***Enhanced efficiency.*** Companies that employ CFD have better insights into their processes. This enables them to operate their equipment at lower cost, potentially reduce emissions and delay unwanted maintenance. Using the additional insight from CFD, plant operators can reduce material waste tremendously.

Within the chemical industry, engineers focus on reducing the time and effort required to develop new processes or redesign or retrofit existing equipment. Achieving this while the plant is in production can be prohibitively expensive and disrupt plant operations. However, this can be accomplished offline virtually with CFD.

## High-performance computing

As with other aspects of engineering, CFD offers varying levels of fidelity. As the complexity of the problem increases, engineers may use more computational points or look at transient aspects of a given problem. Advanced CFD tools provide different modeling capabilities that can run on anything from a standard laptop to a high-performance computing (HPC) system. Leveraging highly scalable HPC unlocks virtually unlimited compute capacity. This enables engineers to rapidly run complex, large model, high-fidelity CFD simulations, perform parametric studies and remove any restrictions that could compromise a design, cutting months off development cycles

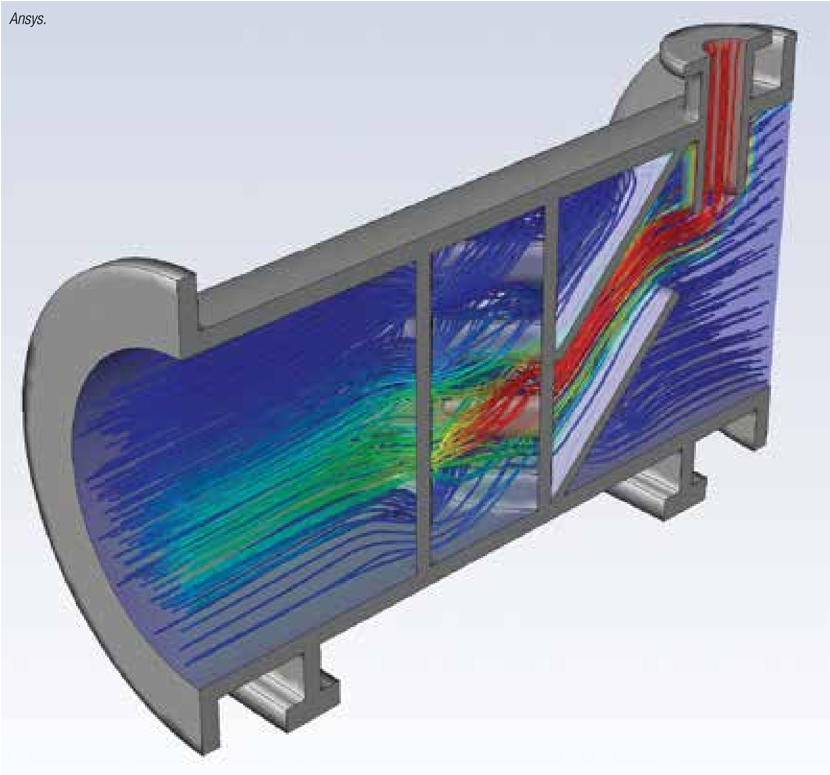


**FIGURE 3.** This diagram shows a visualization of the flow through a static mixer with hot and cold fluids

and expediting the launch of new products. According to an internal study, computing power limitations cause 90% of businesses that run simulations to make modeling concessions by limiting the size of their meshes or making physics models less complicated so they can be completed quickly to meet tight schedules.

*According to an internal study, computing power limitations cause 90% of businesses that run simulations to make modeling concessions in order to meet tight schedules*

HPC computing eliminates those constraints, allowing engineers to generate and analyze computationally difficult simulations using hundreds of compute cores to gain additional insight into their design's performance. Utilizing affordable distributed hardware instead of costly workstations to create their simulations, engineers can view their results in a couple of hours instead of traditionally needing to wait a full day. Additionally, through parametric optimization, engineers can quickly review numerous design variations to select an optimum design.

The HPC hardware itself may be physical (on premise), in the cloud or a combination of both, depending on the local engineering workload and the site's information technology (IT) infrastructure.

## Advanced CFD software

Tasked with accomplishing more in less time, engineers are turning to leading software providers for enhanced CFD solutions. Equipped with built-in automation of a task-based workflow, cutting-edge CFD software can boost user productivity by reducing the learning curve, decreasing probability of human error and reducing human input. Complicated models that formerly required days or weeks to mesh now require only hours, and still deliver high simulation accuracy. Additionally, engineers can obtain answers to their design questions sooner, while also exploring a larger variety of design options in the same timeframe as before.

CFD continues to slash design cycles, reduce costs and drive unprecedented innovation. Disrupting the status quo of product development, CFD enables engineers with next-generation capabilities to create highly accurate designs that increase production flows, improve stability, promote sustainability and significantly improve processes. As engineers continue to harness the powerful capabilities of HPC and new CFD software, complex models are solved faster than ever, enabling companies to deliver new products to market with unmatched speed. ■

*Edited by Scott Jenkins*

## Author

**Hossam Metwally** is a principal application engineer at Ansys Inc. (2600 Ansys Drive, Canonsburg, PA 15317; Phone: 844.462.6797; Email: hossam.metwally@ansys.com). In his current role, Metwally leads a group of engineers focusing on business development for the chemicals, power, pharmaceuticals and consumer products industries. Metwally is involved in technical and sales support, training, technical marketing, testing, documentation revisions and business development for chemicals, rubber, glass and polymer processing companies. He obtained a Ph.D. in mechanical engineering from the University of Cincinnati in 2002. Metwally joined the consulting group in Fluent, Inc. (now part of Ansys Inc.) in 2001.

Part 2

# Portable CFD: Build Interpolation Models from CFD results

Portable laptop computers and smartphones can be used to emulate computational fluid dynamics (CFD) modeling results using this interpolation procedure

**Joseph Colannino**
Colannino Consultants LLC

## IN BRIEF

STATISTICAL EXPERIMENTAL DESIGN

REGRESSING SPATIAL RESPONSES

INCLUDING CATEGORICAL FACTORS

Most engineers are familiar with computational-fluid-dynamics (CFD) models and their power (for an overview of CFD, see Part 1, p. 28). At their best, CFD simulations allow engineers to accurately emulate process equipment and to generate useful results where traditional experimentation may be cost-prohibitive or even impossible. Moreover, CFD can produce stunning visual maps and insights for flow fields that cannot be achieved by any other kind of modeling.

While CFD requires serious computational hardware that is well beyond the means of portable computers, once the CFD model has been created, interpolating models can precisely emulate CFD results in laptops for feed-forward algorithms and distributed control system (DCS) controls, or even smartphones. To generate interpolating models, virtual experiments are conducted over a balanced range of "what-if" scenarios using statistical experimental design (SED) to generate a mathematical French curve — that is, a precision interpolating model. The term "virtual experiment" means collecting the results of CFD or simulator outputs as a function of changes to model inputs, rather than from actual experiments in the real world. Within the desired "factor space," the interpolating model accurately emulates the CFD results. This article describes how to build such interpolating models from CFD or other simulation results.

### Statistical experimental design

SED correlates output variables (termed responses) with input variables (called factors). The general relation of a response to a series of factors (referred to as the factor space) is known as a response surface. To build it, one interrogates the response in factor space, collects the responses, and then fits an interpolating model via a basic five-step procedure.

***Step 1.*** Decide which factors and factor ranges are of interest

***Step 2.*** Select an experimental design

***Step 3***. Perform virtual experiments by interrogating validated CFD or simulation software

***Step 4.*** Use the virtual results to create an interpolating model

***Step 5.*** Confirm the fit of the interpolating model to the simulation results

To illustrate the procedure, we will use an example problem involving furnace temperature in a petroleum refinery heater. The objective of this modeling and interpolation exercise will be to correlate the furnace temperature at the exit of the radiant section (the so-called bridgewall temperature, or BWT) as the hydrogen content in the refinery fuel ($\xi_1$) varies between 25 and 50%, and the oxygen concentration in the fluegas ($\xi_2$) varies between 1.7 and 2.3%.

***Step 1. Factors and ranges of interest.*** The two factors of interest are $\xi_1$ and $\xi_2$, and the response is the BWT. The ranges of interest are 25% ≤ $\xi_1$ ≤ 50% and 1.7% ≤ $\xi_2$ ≤ 2.3%. This defines an implicit functional model, such that:

$$y = f(\xi_1, \xi_2) \quad \textbf{(1)}$$

Here, $y$ is the response of interest, which, in this case, is the BWT. The BWT depends on many interrelated factors, including the following: heat flux in the furnace; the combustion environment and flame dynamics; the properties of the process fluid; the fluid phases and flow regimes in the furnace tubes; and others. In short, a closed-form mathematical model from first principles is intractable. Notwithstanding, and presuming that the explicit form of the true (but un-

| TABLE 1. BWT AS A FUNCTION OF $H_2$ AND $O_2$ | | |
|---|---|---|
| $H_2$, % | $O_2$, % | BWT, °F |
| 25.0 | 1.7 | 1,640 |
| 37.5 | 1.7 | 1,650 |
| 50.0 | 1.7 | 1,660 |
| 25.0 | 2.0 | 1,790 |
| 37.5 | 2.0 | 1,800 |
| 50.0 | 2.0 | 1,810 |
| 25.0 | 2.3 | 1,890 |
| 37.5 | 2.3 | 1,902 |
| 50.0 | 2.3 | 1,905 |

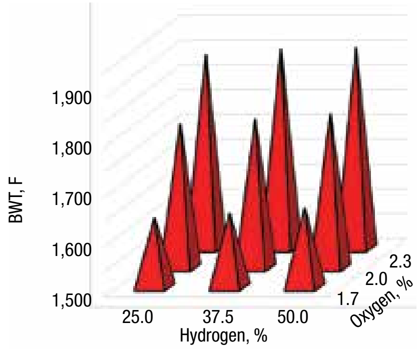


**FIGURE 1.** This graphs shows BWT as a function of $H_2$ and $O_2$. In this case, BWT is seen to be a stronger function of oxygen concentration in the fluegas and a weaker function of fuel hydrogen concentration

knowable) model is smooth (as is the general case for macroscopic engineering phenomena), we may approximate the unknown model with a Taylor series. With an appropriate scale transformation (from ξ to *x*, as described here), we may express Equation (1) with a simpler Maclaurin series (that is, a Taylor series centered at zero).

$$y = g(x_1,x_2) = g(0,0) + \left(\frac{\partial y}{\partial x_1}\right)x_1 + \left(\frac{\partial y}{\partial x_2}\right)x_2 + \left[\frac{1}{2!}\left(\frac{\partial^2 y}{\partial x_1^2}\right)\right]x_1^2 + \left(\frac{\partial^2 y}{\partial x_1 \partial x_2}\right)x_1 x_2 + \left[\frac{1}{2!}\left(\frac{\partial^2 y}{\partial x_2^2}\right)\right]x_2^2 + \cdots \quad (2)$$

At first blush, this may not seem like progress. If we do not know $g(x_1,x_2)$ explicitly, how can we know its partial derivatives? But in fact, they may be found numerically. Letting $a_0 = g(0,0)$, and $a_1 = (\partial y/\partial x_1)$, $a_2 = (\partial y/\partial x_2)$, and so on, we can obtain the following series, shown in Equation (3).

$$y = g(x_1,x_2) = a_0 + a_1x_1 + a_2x_2 + a_{11}x_1^2 + a_{12}x_1x_2 + a_{22}x_2^2 + \ldots \quad (3)$$

For the time being, let us presume that Equation (3) may be truncated at $a_{22}x_2^2$ without significant loss of accuracy. In that case, Equation (3) would reduce to Equation (4), where an error term (ε) cumulates the sum of the terms after $a_{22}x_2^2$.

$$y = a_0 + a_1x_1 + a_2x_2 + a_{11}x_1^2 + a_{12}x_1x_2 + a_{22}x_2^2 + \varepsilon \quad (4)$$

We shall designate the truncated model by $\hat{y}$; so that by definition,

$$\varepsilon \equiv y - \hat{y} \quad (5)$$

***Step 2. Experimental design.*** A factorial design [1] interrogates the factor space in a uniform way and requires *n* virtual experiments, where

$$n = L^{n_f} \quad (6)$$

Here, *L* represents the number of different levels we wish to investigate for each factor and $n_f$ is the number of factors. Since Equation (4) has six adjustable parameters ($a_0$, $a_1$, $a_2$, $a_{11}$, $a_{12}$ and $a_{22}$), we need at least six virtual experiments to fit them. Ideally, we should run more interrogations in order to assess the lack of fit (or error ε) caused by terminating the model after a finite number of terms. In our case, we have two factors ($\xi_1$ and $\xi_2$). If we use only two levels for each factor, we will only run $2^2 = 4$ virtual experiments. This is too few for our needs. So, we shall use a three-level factorial design [2] requiring $3^2 = 9$ virtual experiments. The design uses equidistant factor levels (that is, $O_2$ = 1.7%, 2.0%, 2.3%, $H_2$ = 25.0%, 37.5%, 50%).

***Step 3. Virtual experiments.*** Figure 1 shows the results of the virtual experiments for each of the nine coordinates in the factor space. Now we must adjust the coefficients of Equation (4) to accurately represent the data shown in Table 1, and provide for smooth and continuous interpolation between and among the points.

Replicate simulations will generate no pure error because replicate points will always produce exactly the same result. Therefore, our source of error (ε) in Equation (4) will be exclusively from the lack of fit caused by the truncation of the model and collected in ε. The central-limit theorem of statistics [3] says that disparate effects from a large collection of extraneous sources will tend toward a normal (that is, Gaussian) distribution. If ε is normally distributed [4], the best method for determining the coefficients is to adjust them in a way that minimizes the sum of the squared errors (also known as the method of least squares). That is, *n* data points give *n* associated errors ($\varepsilon_1$, $\varepsilon_2$, … $\varepsilon_n$). For the case at hand, *n* = 9, and is indexed by *k* = 1, 2, … 9 in Equation (7a).

$$y_k = a_0 + a_1x_{1,k} + a_2x_{2,k} + a_{11}x_{1,k}^2 + a_{12}x_{1,k}x_{2,k} + a_{22}x_{2,k}^2 + \varepsilon_k \quad (7a)$$

Next, adjust $a_0$ … $a_{22}$ such that

**DATA TABLE**

| $H_2$, % | $O_2$, % | BWT, °F | $\hat{y}$ |
|---|---|---|---|
| 25.0 | 1.7 | 1640 | 1,639 |
| 37.5 | 1.7 | 1650 | 1,651 |
| 50.0 | 1.7 | 1660 | 1,660 |
| 25.0 | 2 | 1790 | 1,790 |
| 37.5 | 2 | 1800 | 1,801 |
| 50.0 | 2 | 1810 | 1,809 |
| 25.0 | 2.3 | 1890 | 1,891 |
| 37.5 | 2.3 | 1902 | 1,900 |
| 50.0 | 2.3 | 1905 | 1,906 |

**X**

| 0 | 1 | 2 | 11 | 12 | 22 |
|---|---|---|---|---|---|
| 1 | -1 | -1 | 0.33333 | 1 | 0.33333 |
| 1 | 0 | -1 | -0.6667 | 0 | 0.33333 |
| 1 | 1 | -1 | 0.33333 | -1 | 0.33333 |
| 1 | -1 | 0 | 0.33333 | 0 | -0.6667 |
| 1 | 0 | 0 | -0.6667 | 0 | -0.6667 |
| 1 | 1 | 0 | 0.33333 | 0 | -0.6667 |
| 1 | -1 | 1 | 0.33333 | -1 | 0.33333 |
| 1 | 0 | 1 | -0.6667 | 0 | 0.33333 |
| 1 | 1 | 1 | 0.33333 | 1 | 0.33333 |

**$X^TX$**

| 0 | 1 | 2 | 11 | 12 | 22 |
|---|---|---|---|---|---|
| 9 | 0 | 0 | 0 | 0 | 0 |
| 0 | 6 | 0 | 0 | 0 | 0 |
| 0 | 0 | 6 | 0 | 0 | 0 |
| 0 | 0 | 0 | 2 | 0 | 0 |
| 0 | 0 | 0 | 0 | 4 | 0 |
| 0 | 0 | 0 | 0 | 0 | 2 |

**$(X^TX)^{-1}$**

| 0 | 1 | 2 | 11 | 12 | 22 |
|---|---|---|---|---|---|
| 0.11111 | 0 | 0 | 0 | 0 | 0 |
| 0 | 0.16667 | 0 | 0 | 0 | 0 |
| 0 | 0 | 0.16667 | 0 | 0 | 0 |
| 0 | 0 | 0 | 0.5 | 0 | 0 |
| 0 | 0 | 0 | 0 | 0.25 | 0 |
| 0 | 0 | 0 | 0 | 0 | 0.5 |

| $X^Ty$ | Coeff. | a | ± | S.E. |
|---|---|---|---|---|
| 16047 | $a_0$ | 1,783.0 | ± | 0.6 |
| 55 | $a_1$ | 9.2 | ± | 0.8 |
| 747 | $a_2$ | 124.5 | ± | 0.8 |
| -3 | $a_{11}$ | -1.5 | ± | 1.4 |
| -5 | $a_{12}$ | -1.3 | ± | 1.0 |
| -51 | $a_{22}$ | -25.5 | ± | 1.4 |

**GENERAL ANOVA**

| | EFFECT | SS | DF | MS | F | p | |
|---|---|---|---|---|---|---|---|
| * | M | 94816.9 | 5 | 18963.4 | 5132.95 | 4.3E-06 | * |
| | R | 11.0833 | 3 | 3.69444 | s | 1.92209 | |
| | T | 94828 | 8 | | $R^2$ | 0.99988 | |

**DETAILED ANOVA**

| | EFFECT | SS | DF | MS | F | p | $R^2$ | |
|---|---|---|---|---|---|---|---|---|
| * | $x_1$ | 504.167 | 1 | 504.167 | 136.466 | 0.00135 | 0.00532 | * |
| * | $x_2$ | 93001.5 | 1 | 93001.5 | 25173.3 | 5.5E-07 | 0.98074 | * |
| | $x_1^2$ | 4.5 | 1 | 4.5 | 1.21805 | 0.35032 | 4.7E-05 | |
| | $x_1x_2$ | 6.25 | 1 | 6.25 | 1.69173 | 0.28427 | 6.6E-05 | |
| * | $x_2^2$ | 1300.5 | 1 | 1300.5 | 352.015 | 0.00033 | 0.01371 | * |
| | R | 11.0833 | 3 | 3.69444 | s | 1.92209 | | |
| | T | 94828 | 8 | | $R^2$ | 0.99988 | 0.99977 | * |

**CALCULATION DETAILS**

- SSM = $\hat{y}^T\hat{y} - \bar{y}^T\bar{y}$ = MMULT(TRANSPOSE(F3:F11),E3:E11) – COUNT(D3:D11)*(AVERAGE(D3:D11)^2)
- SSR = $y^Ty - \hat{y}^T\hat{y}$ = MMULT(TRANSPOSE(E3:E11),E3:E11) – MMULT(TRANSPOSE(F3:F11),F3:F11)
- SST = $y^Ty - \bar{y}^T\bar{y}$ = MMULT(TRANSPOSE(D3:D11),D3:D11) – COUNT(D3:D11)*(AVERAGE(D3:D11)^2)
- $X^TX$ = MMULT(TRANSPOSE(G3:L11),G3:L11)
- $X^Ty$ = MMULT(TRANSPOSE(G3:L11),D3:D11)
- $(X^TX)^{-1}$ = MINVERSE(N3:S8) | $\hat{y} = Xa$ = MMULT(G3:G11,W3:W8)
- $SSx_1 = a_1(X^Ty)_1$ = U4*W4
- $SSx_2 = a_2(X^Ty)_2$ = U5*W5
- $SSx_1^2 = a_{11}(X^Ty)_{11}$ = U6*W6
- $SSx_1x_2 = a_{12}(X^Ty)_{12}$ = U7*W7
- $SSx_2^2 = a_{22}(X^Ty)_{22}$ = U8*W8
- DFM = $n_f - 1$ = COUNT(G2:L2) – 1
- DFT = $n - 1$ = COUNT(D3:D11) – 1
- DFR = $n - n_f$ = DFT - DFM = COUNT(D3:D11) – COUNT(G2:L2)
- MSM = SSM/DFM = C15/D15
- MSR = SSR/DFR = C16/D16
- $a = (X^TX)^{-1} * X^Ty$ = MMULT(N12:S17,U3:U8)
- $SEx_k = \sqrt{[(X^TX)^{-1}_{k,k} * MSR]}$; e.g., $SEx_1$ = SQRT(O13*E16)
- F = MSM/MSR = E15/E16
- $F_k = MSx_k/MSR$; e.g., $F_1$ = E21/E26
- $R_k^2 = SSx_k/SST$; e.g., $SSx_1$ = C21/C27
- $R^2$ = SSM/SST = C15/C17
- p = FDIST(DFM,DFR,F) = FDIST(D15,D16,F15)
- $p_k$ = FDIST($DF_1$,DFR,$F_k$); e.g., $p_1$ = FDIST(D21,D26,F21)
- s = $\sqrt{MSR}$ = SQRT(E16)

**FIGURE 2.** The figure shows the formulas in the spreadsheet for all necessary calculations and their results

$\sum_{k=1}^{9}\varepsilon^2_k$ —>min.

***Step 4. Creating the interpolating model.*** Expressing Equation (7a) in matrix form [5] for each result gives Equation (7b), where the rightmost subscript of $y$, $x$ and $\varepsilon$ indexes each one for each data point.

$$\begin{pmatrix} y_1 \\ y_2 \\ \vdots \\ y_9 \end{pmatrix} = \begin{pmatrix} 1 & x_{1,1} & x_{2,1} & x_{1,1}^2 & x_{1,1}x_{2,1} & x_{2,1}^2 \\ 1 & x_{1,2} & x_{2,2} & x_{1,2}^2 & x_{1,2}x_{2,2} & x_{2,2}^2 \\ \vdots & \vdots & \vdots & \vdots & \vdots & \vdots \\ 1 & x_{1,9} & x_{2,9} & x_{1,9}^2 & x_{1,9}x_{2,9} & x_{2,9}^2 \end{pmatrix} \begin{pmatrix} a_0 \\ a_1 \\ a_2 \\ a_{11} \\ a_{12} \\ a_{22} \end{pmatrix} + \begin{pmatrix} \varepsilon_1 \\ \varepsilon_2 \\ \vdots \\ \varepsilon_9 \end{pmatrix} \quad \textbf{(7b)}$$

A more compact way of representing Equation (7b) is shown by Equation (7c).

$$\boldsymbol{y} = \boldsymbol{Xa} + \varepsilon \quad \textbf{(7c)}$$

Equations (7a), (7b) and (7c) are all equivalent formulations. In Equation (7c), bold lower-case letters indicate the respective column vectors (having rows but only one column) and the bold upper-case letter indicates the respective matrix (having both rows and columns). It turns out that finding $\sum_{k=1}^{n} \varepsilon_k^2$ —> min for the $m$ coefficients of Equation (4) is equivalent to pre-multiplying Equation (7c) by its transpose, $\boldsymbol{X}^T$, and solving for $\boldsymbol{a}$ [6].

$$\boldsymbol{X^Ty} = (\boldsymbol{X^TX})\boldsymbol{a}; \qquad \boldsymbol{a} = (\boldsymbol{X^TX})^{-1}\boldsymbol{X^Ty} \quad \textbf{(8a, b)}$$

Here, the superscript $T$ is the transpose operator, which switches rows and columns. This bit of housekeeping is necessary, since matrix algebra requires that column elements multiply row elements). The superscript $^{-1}$ of Equation (8b) denotes the inverse matrix. Fortunately, spreadsheet programs such as Microsoft Excel capably solve matrix equations. The Excel command for the transpose operator is =TRANSPOSE(X). The inverse is implemented as =MINVERSE($X^TX$). Figure 2 shows the spreadsheet containing all the formulas and results.

Cells B2:D11 hold the Figure 1 data. Next, we establish the $\boldsymbol{X}$ matrix of Equation (7b) in cells G1:L11. Per Equation (7b), the first column (labeled 0) is a column of units. The second and third columns (labeled 1 and 2) hold coded values for $\xi_1$ and $\xi_2$ (cells G3:L11), as given by Equation (9).

$$x_k = (\xi_k - \bar{\xi}_k) / (\tilde{\xi}_k/2)$$
$$x_1 = (\xi_1 - 37.5\%)/(12.5\%)$$
$$x_2 = (\xi_2 - 2.0\%)/(0.6\%) \quad \textbf{(9a, b, c)}$$

These coding transforms ($x_k$) are merely $\xi_k$ offset by the mean ($\bar{\xi}_k$) and normalized by the half range ($\tilde{\xi}/2$) = (max$\xi_k$ – min$\xi_k$)/2. The regression gives equivalent results whether or not the factors are coded. However, such coding centers the factors at 0 and scales the respective factor ranges to a non-dimensional ±1. This transforms the truncated Taylor series to a Maclaurin series and makes the coefficients easier to compare. The next three columns of the matrix (cells J3:L11) are derived from the values of 1 and 2. However, the observant reader will note that the squares of the coded factors (labeled 11 and 22 in J3:J11 and L3:L11, respectively) have been offset by 2/3. The quadratic offset, which will be called $m_2$ in this article, is the mean square of the particular factor value, $m_{2,j} \equiv (\sum_{k=1}^{n} x_{j,k}^2)/n$, which for this 32-factorial design, happens to be 2/3 for both $x_1^2$ and $x_2^2$. These two adjustments — the coding transforms and the quadratic offsets — cause the non-diagonal elements of $\boldsymbol{X^TX}$ (cells N3:S8) to vanish, thus rendering each coefficient linearly independent. These adjustments represent a slight modification of Equation (4) to give Equation (10).

$$y = a_0 + a_1x_1 + a_2x_2 + a_{11}\,(x_1^2 - {}^2/_3) + a_{12}x_1x_2 + a_{22}\,(x_2^2 - {}^2/_3) + \varepsilon \quad \textbf{(10)}$$

Equations (10) and (4) are essentially the same, except that $a_0$ in Equation (4) has been distributed as $a_0 - {}^2/_3\,(a_{11} + a_{22})$ in Equation (10). However, a regression on Equation (10) in lieu of Equation (4) has two advantages. First, one may perform statistical tests on each coefficient independently. Second, if some coefficients are statistically or practically insignificant, one may drop them from the model without having to recalculate those remaining.

To calculate $\boldsymbol{X^TX}$ from $\boldsymbol{X}$, use the Excel command =MMULT(TRANSPOSE(X), X). Per Equation (8b), the

| $H_2$, % | $O_2$, % | BWT, ºF | ŷ |
|---|---|---|---|
| 25.0 | 1.7 | 1,640 | 1,639 |
| 37.5 | 1.7 | 1,650 | 1,651 |
| 50.0 | 1.7 | 1,660 | 1,660 |
| 25.0 | 2 | 1,790 | 1,790 |
| 37.5 | 2 | 1,800 | 1,801 |
| 50.0 | 2 | 1,810 | 1,809 |
| 25.0 | 2.3 | 1,890 | 1,891 |
| 37.5 | 2.3 | 1,902 | 1,900 |
| 50.0 | 2.3 | 1,905 | 1,906 |

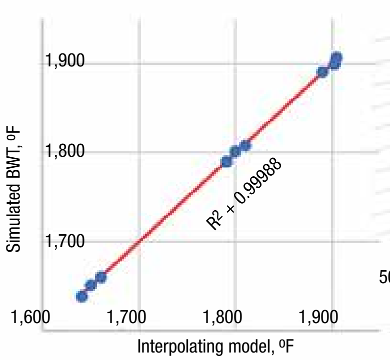


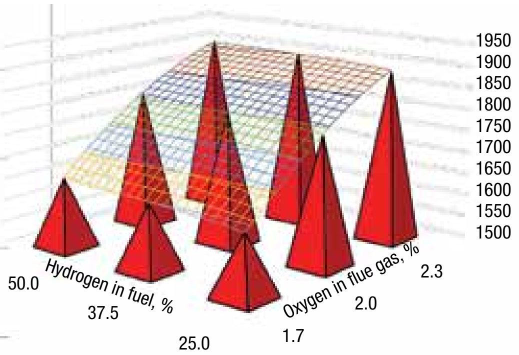


**FIGURE 3.** The diagram compares the original simulation with the interpolating model. The interpolating model gives the simulation results to within a degree or two Fahrenheit (left panel). The middle panel displays the same results graphically. A perfect fit of the data would have resulted in an $R^2 = 1$ and all data lying on the red line. The right panel shows the interpolating model (contoured mesh) overlaid on the original data set

coefficient vector, ***a*** (cells W4:W9), derives from two matrices: the inverse matrix, $(\boldsymbol{X^TX})^{-1}$ =MINVERSE($X^TX$); cells N12:S17; and an intermediate vector, $\boldsymbol{X^Ty}$ (U3:U8) =MMULT(TRANSPOSE(X). Then, $\hat{y} = \boldsymbol{Xa}$ (E3:E11) =MMULT(***X,a***).

***Step 5. Assessing the interpolating model.*** Figure 3 shows that the interpolating model ($\hat{y}$) emulates the simulation results ($y$ = BWT) within a degree or two Fahrenheit. While not perfect, the interpolating model is adequate for the task. Indeed, we could have made our model perfect by fitting a nine-coefficient model instead of the six-coefficient one. However, not even all six of the determined coefficients are statistically significant, so there is no need to expand the model to include higher-order terms. An analysis of variance (ANOVA) will show which coefficients are significant and which are not.

We report two ANOVAs in Figure 2 — a general ANOVA (B13:G17), applicable to any data set — and a detailed ANOVA (B19:H27), applicable only to orthogonal data sets [7] such as ours. The ANOVA contains various sums of squares (SS) to apportion the total variance (SST) among the model (SSM) or model components ($SSx_1$, $SSx_2$, and so on) and the residual error (SSR). Calculating the ratio between the mean square (MS) of the model (MSM) or model components ($MSx_1$, $MSx_2$, and so on) and dividing by the mean square residual (MSR) results in respective $F$ ratios. In turn, those ratios can be referenced against theoretical $F$ distributions to calculate the probability ($p$) that the model does not differ from the error. For example, $p < 0.05$ (a common threshold) denotes greater than 95% confidence that the term is statistically significant. The ANOVA also allows the calculation of a coefficient of determination ($R^2$= SSM/SST). When $R^2 = 1$, the interpolating model fits the data perfectly. For orthogonal models, one may also calculate the fraction of the variance of each term in Equation (10) to measure practical significance (that is $R_1^2 + R_2^2 + \ldots + R_{22}^2 = R^2$ ; cells H21:H27); which is the influence each term has on conforming the interpolation model to the response.

The detailed ANOVA shows that only the $x_1$, $x_2$, and $x_1^2$ effects are significant as indicated by $p \leq 0.05$ (cells G21:G25). For convenience, there is an asterisk beside each significant effect in Figure 2 (A21:A25 or I21:I25). From this analysis, the full model of Equation (10) ($R^2$ = 0.99988) is not appreciably better than the four-term model of Equation (11) ($R^2$ = 0.99977), which is preferred.

$$y = a_0 + a_1x_1 + a_2x_2 + a_{22}\,(x_2^2 - {}^2/_3) + \varepsilon \quad \textbf{(11)}$$

The ANOVA also allows calculation of the standard deviation for the $\hat{y}$ values. In our case, $s = \sqrt{\text{MSR}} = \pm 1.92$ºF (G26). The standard errors (SE) give the respective deviations for the coefficients themselves (Y3:Y8) and also support the truncated model of Equation (11).

**FIGURE 4.** This graphs shows the normalized heat-flux profile. This is a particular normalized heat flux (curve) for a particular set of factors and sampled at 21 elevations (points). In this example, the maximum heat flux occurs just below the mid-point of the heater elevation at about 47%

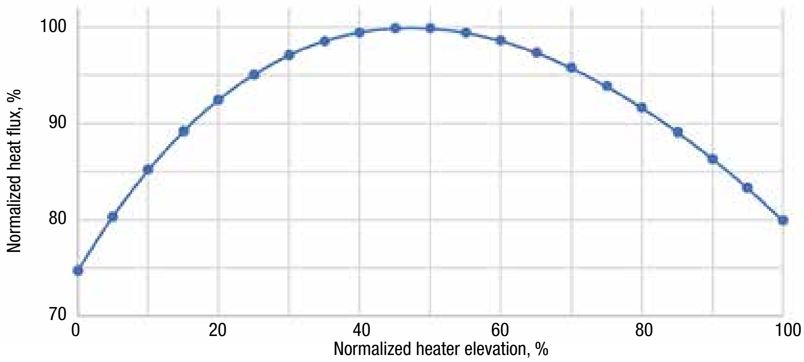

At this point, we have concluded Step 5 and the current example.

## Regressing spatial responses

So far, so good. But BWT is a point-local response — that is, it is zero dimensional (0D), existing at a single location in the heater. Often in CFD simulations, the responses of interest are not localized, but span one or more dimensions. For example, velocity vectors, temperatures, or pressure gradients may be associated with one-, two- or three-dimensional spaces. To keep the treatment from growing overly complicated, the article illustrates the method for a 1D response. Nonetheless, the method generalizes to 2D or 3D problems.

Consider the normalized heat flux ($\phi$) in the furnace of an ethylene reactor as a function of normalized elevation in the heater (Figure 4).

Heat flux in the furnace is affected by the burner type, fuel composition, fuel pressure, fuel flowrate, oxygen concentration in the fluegas, runtime history, and many other factors. It is possible to include all such factors in an interpolating model. However, to illustrate the method, it will be sufficient to consider $\phi$ as a function of two factors: oxygen in the fluegas ($\xi_1$) and the run time ($\xi_2$), coded to $x_1$ and $x_2$ in the same way as indicated in Equation (9a).

$$\phi = f(\xi_1,\xi_2) + \varepsilon = g(x_1,x_2) + \varepsilon$$
$$\hat{\phi} = f(\xi_1,\xi_2) = g(x_1,x_2) \qquad \textbf{(12a, b)}$$

At the start of run (SOR, $\xi_2 = 0$) the tubes are clean, but weeks later, near the end of run (EOR, $\xi_2 = 1$), the tubes have become fouled, and fouling affects the heat-flux profile. For assessing the effect of oxygen and runtime on $\phi$, we shall once again use a $3^2$-factorial design. The interpolating model is more complicated than before because each point in factor space is associated with an entire heat-flux profile, not just a point measurement. Rather than perform a regression on $3^2 \times 21 = 189$ sample points, we shall modify Step 4 and transform the heat flux from the spatial domain to a polynomial domain using

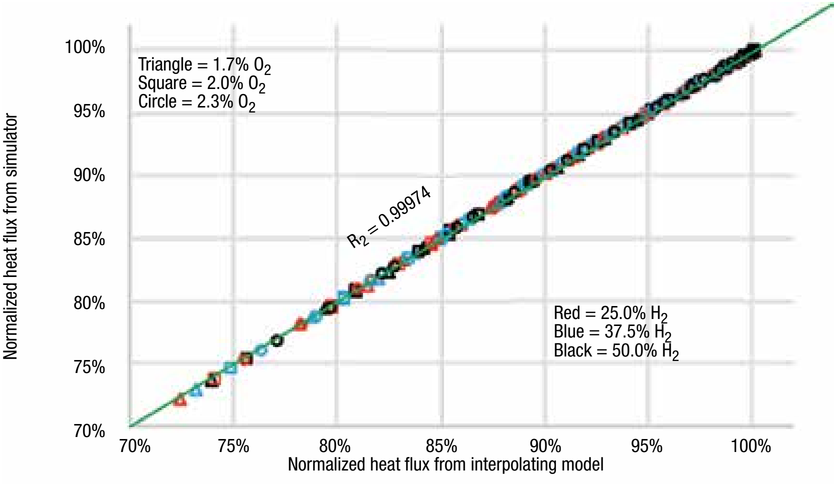


**FIGURE 5. The graph shows a comparison of the simulation and interpolating-model results. The interpolating model adequately represents the output of the full-order heat-flux simulation**

a discrete form of a Legendre polynomial [8]. In particular, we shall transform the heat flux as a function of distance $\phi(z)$ to a function of polynomial space $\phi(c)$, which, for the case at hand, will be a cubic polynomial [9] comprising four coefficients ($c_0$, $c_1$, $c_2$, and $c_3$) in lieu of the 21 samples of $z$. To do this, we will regress each of $3^2 = 9$ heat flux profiles using Equation (13), indexed by $k = 1, 2, \ldots 9$.

$$\phi_k(z) = c_{0,k} + c_{1,k}z + c_{2,k}(z^2 - m_2) + c_{3,k}(z^3 - m^3 z) \quad \textbf{(13)}$$

Here, $z$ is the coded elevation (–1 to +1) sampled at 21 locations, $m_2 = (\sum_{h=1}^{21} z_h^2)/21$, and $m_3 = (\sum_{h=1}^{21} z_h^4)/(\sum_{h=1}^{21} z_h^2)$. Equation (13) is the discrete form of a Legendre polynomial. It is a typical cubic polynomial, except that the offsets $m_2$ and $m_3$ keep all the coefficients independent. This is the same trick we used in deriving the quadratic offset of Equation (10), except that now we have a cubic offset as well. We then regress $c_0$, $c_1$, $c_2$ and $c_3$ as responses in $x_1$-by-$x_2$ factor space.

$$c_{j,k} = a_{0,j} + a_{1,j}x_1 + a_{2,j}x_2 + a_{11,j}(x_1^2 - {}^2/_3) + a_{12,j}x^1x_2 + a_{22,j}(x^2{}_1 - {}^2/_3) + \varepsilon \quad \textbf{(14)}$$

Here, $k = 1, 2, \ldots 9$ indexes the particular heat flux profile, and $j = 0, 1, 2, 3$ indexes each Legendre coefficient response. This double indexing results in $9 \times 4 = 36$ $c_{j,k}$ coefficients. These are then substituted into Equation (13) to obtain our final relation, as shown in Equation (15).

$$\Phi(x_1, x_2, z) = c_{0,k}(x_1,x_2) + c_{1,k}(x_1,x_2)z + c_{2,k}(x_1,x_2)(z^2 - m_2) + c_{3,k}(x_1,x_2)(z^3 - m_3 z) \quad \textbf{(15)}$$

Step 5 generates the usual intermediate statistics already described. The final $R^2$ is assessed by comparing the 189 outputs of the simulation against the interpolating model of Equation (15). Figure 5 shows the fit.

The technique may be adjusted for two-dimensional or three-dimensional problems [*10*]. While it is true that 2D and 3D models will generate more coefficients, even this larger number will remain well within the capabilities of a typical spreadsheet or laptop.

## Including categorical factors

Results may be collected from a CFD model run at a variety of conditions with little additional trouble. However, changes in geometry are altogether different. Changing a burner, adding a baffle, or making some other geometric change to the model will require regridding of the mesh, and that is not a trivial task. However, with forethought, one may build a baffle or something similar into the original CFD model and toggle the object on or off. This is represented in the interpolating function by a categorical factor — coded, for example, as –1 = baffle omitted, +1 = baffle included.

A categorical factor is one that is not continuous, but that has particular states, such as on/off, up/down, position 1, 2, 3, and so on. For example, if a damper is restricted to five positions from closed to open (for example, 0%, 25%, 50%, 75%, 100% open), then Equation (9a) gives the respective coding (–1, –½, 0, ½, 1). If these are included as part of the original CFD model, then various combinations in factor space are relatively easy to assess and may be expressed via categorical factors in the interpolating model.

Interpolated results for the models presented are quite good (and may be made as good as desired). However, there is an important note of caution: extrapolation outside of the original factor space is never warranted. This is because interpolating models are made compact precisely by discarding the higher-order terms of the Maclaurin series. Inside the factor space, these terms exert a negligible influence on the response, as the error statistics affirm. However, outside the factor space, the discarded terms

grow exponentially and wreck the results. Otherwise, the method described here can squeeze computationally-intensive simulation results into interpolating models. Such models are suitable for spreadsheets or programs, to be run on laptops, or to be put into control systems for use in feed-forward control or diagnostic reporting. ■

*Edited by Scott Jenkins*

## References and end notes


1. For more about factorial designs, see Colannino, J., "Modeling of Combustion Systems, A Practical Approach," Taylor and Francis, Boca Raton, Fla., 2006, chapters 1 and 3. For general works on factorial designs and response surface methodology, see the book by Box, G.E.P and Draper, N.R., "Interpolating Model-Building and Response Surfaces," John Wiley & Sons, New York, 1987. A more recently published treatment is given in Montgomery, D.C., "Design and Analysis of Experiments," John Wiley & Sons, 2019.
2. Factorial designs may be fractionated in a variety of ways and there are many other experimental designs in the statistician's tool kit such as simplex designs, central composites, Box-Behnken designs, and so on. The Box-Behnken design was originally reported here: Box, G.E.P. and Behnken, D., Some new three level designs for the study of quantitative variables, *Technometrics*, Vol. 2, pp 455–475, 1960. Colannino (Ref. 1) discusses factorial, fractional factorial, and simplex designs. Also, the NIST Handbook of Statistics www.itl.nist.gov/div898/handbook/) has a section dedicated to the choice of experimental design, www.itl.nist.gov/div898/handbook/pri/section3/pri3.htm, all links last accessed 24 July 2019.
3. See en.wikipedia.org/wiki/central_limit_theorem for more about the central limit theorem, last accessed 22 July 2019.
4. It is possible to test this assumption by plotting the residual error in Excel, or on normal probability paper. For more about the Excel procedure, see blog.excelmasterseries.com/2015/02/normal-probability-plot-with-adjustable.html, last accessed 23 July 2019. www.itl.nist.gov/div898/handbook/eda/section3/normprpl.htm explains the procedure in general, last accessed 26 July 2019.
5. For more about matrix algebra, see R. Bronson, "Schaum's Outline of Matrix Operations" (Schaum's Outline Series), 4th ed., McGraw Hill, New York, 2011 or Colannino (Ref. 1), chapter 1.
6. This is so because to minimize the sum of the squares, we set the partial derivative to zero with respect to each coefficient $\partial/(\partial_{aj})\sum\boldsymbol{\varepsilon}^2 = 0 = \partial/(\partial_{aj})\sum(y-\hat{y})^2$. Since only $\hat{y}$ has adjustable parameters, this reduces to $\sum y(\partial\hat{y}/\partial_{aj}) = \sum \hat{y}(\partial_{\hat{y}}/(\partial_{aj})$, which for any form of Equation (7) may be expressed in matrix form as (8a).
7. Orthogonal polynomials are given in the mathematical handbook of Abramowicz, M. and Stegun, I., "Handbook of Mathematical Functions: with Formulas, Graphs, and Mathematical Tables," Dover Books, Mineola, NY, 1965. They are also described in Colannino (Ref. 1), pp 83–93.
8. For more on Legendre polynomials, see en.wikipedia.org/wiki/Legendre_polynomials, last accessed 24 July 2019.
9. In this particular case, a cubic polynomial is sufficient to represent the heat flux curve of Figure 4. There is nothing magic about using a cubic polynomial. We may use higher- or lower-order polynomials in one, two, or three dimensions, as fit the occasion. However, in all cases, we use the respective discrete form of the Legendre polynomial.
10. This will require the use of two- or three-dimensional versions of an orthogonal series, such as Legendre polynomials or those of Fourier, Hermite, Chebyshev, and so on. See https://en.wikipedia.org/wiki/Orthogonal_polynomials for more information, last accessed 24 July 2019. Colannino (Ref. 1), pp 80–92 also includes a section on these.


## Author


**Joseph Colannino** is principal and CEO at Colannino Consultants, LLC (Email: colanninoconsultants@gmail.com), a firm specializing in leading process teams to profitable innovation. Colannino is a registered chemical engineer in the state of California with more than 30 years in the hydrocarbon and chemical processing industries. He has more than 100 patents pending and granted, and many of his innovations are still in revenue-producing service. Colannino has authored or co-authored several books in combustion, pollution control, and experimental design. He received his B.S.Ch.E. from the California Polytechnic University at Pomona and holds a M.S. degree in Knowledge Management from the University of Oklahoma with an emphasis in R&D organization. He was formerly head of research and development for John Zink Co., LLC. and CTO for a Seattle-based combustion startup. Now CEO of Colannino Consultants, Colannino consults in combustion and pollution control and teaches industrial courses on experimental design, process optimization, and improving R&D.

Part 1

# Heat Exchangers: Designing for Supercritical Fluid Service

Working with supercritical fluids poses challenges when designing heat exchangers. Some practical tips and precautions are presented here

**James R. Lines**
Graham Corp.

## IN BRIEF

THERMAL DUTY

TEMPERATURE VERSUS THERMAL DUTY

FLUID PROPERTY VARIATION

HEAT-TRANSFER COEFFICIENT

SUMMARY

Industrial applications involving fluids at high pressure — pressure above the critical pressure of a particular fluid — are increasing in number. This is due to the beneficial properties of supercritical fluids (SCFs) or simply due to very high pressures required for certain applications. Examples include supercritical $CO_2$ acting as a solvent in an extraction process, supercritical water for waste treatment via an oxidation process (Figure 1), supercritical nitrogen for an enhanced-oil-recovery process or supercritical methane in compressed natural-gas service. Table 1 provides a list of the critical points for a number of different fluids [*1*]. The phase diagram for $CO_2$, the most commonly used SCF, is shown in Figure 2.

Proper design of heat transfer equipment requires greater care and a deeper understanding of supercritical fluid properties, and in particular, how those properties may vary as temperature changes. This article provides design considerations for heat exchangers in supercritical service in order to achieve reliable process performance.

### Thermal duty

When presented with supercritical design requirements, an initial step is to determine

**TABLE 1. CRITICAL POINTS FOR VARIOUS FLUIDS [*1*]**

| Substance | Temperature | | Pressure | |
|---|---|---|---|---|
| | °F | K | psia | bara |
| Carbon dioxide | 87.9 | 304.2 | 1,071.8 | 73.9 |
| Carbon monoxide | –220.3 | 133 | 507.6 | 35.0 |
| Hydrogen | –399.7 | 33.3 | 188.5 | 13.0 |
| Methane | –115.7 | 191.1 | 673.0 | 46.4 |
| Nitrogen | –232.5 | 126.2 | 491.7 | 33.9 |
| Oxygen | –181.0 | 154.8 | 736.8 | 50.8 |
| Water | 705.5 | 647.3 | 3,203.8 | 220.9 |

Graham

**FIGURE 1. This heat exchanger is used for supercritical water oxidation service. Both hot and cold fluids operate above critical pressure**

the thermal duty of the heat-exchanger, $Q$. Under normal conditions, this is most commonly expressed as Equation (1).

$$Q = \dot{m} \times C_p \times \Delta T \quad (1)$$

Where:
$\dot{m}$ = mass flowrate
$C_p$ = average specific heat capacity
$\Delta T$ = temperature change

It is common for an end user that is requesting a design to provide fluid properties, such as the average heat capacity, at the average temperature. In supercritical service, this can lead to an incorrect determination of thermal duty. Instead, the best practice is to calculate thermal duty considering change in enthalpy, $\Delta h$, as shown in Equation (2).

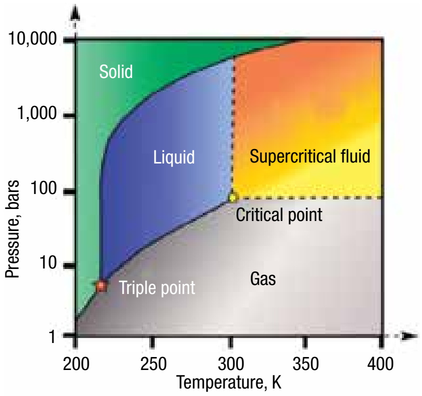


**FIGURE 2. The phase diagram for carbon dioxide illustrates the location of the critical point**

$$Q = \dot{m} \times \Delta h \tag{2}$$

Specific heat can greatly vary with temperature when operating in the supercritical region. For this reason, the change in enthalpy is the most appropriate term for determining the thermal duty. This is best illustrated via an example. Consider a supercritical $CO_2$-extraction application where $CO_2$ at 1,450 psia (1,000 kPa) and a mass flowrate of 11,023 lb/h (5,000 kg/h) must be heated from –10°F to 150°F (–23.3 to 65.6°C). The specific heat capacity of $CO_2$ at the average temperature is 0.637 Btu/lb°F (0.637 kcal/kg°C). The enthalpy at the inlet and outlet temperatures are 63.3 Btu/lb (35.2 kcal/kg) and 189.4 Btu/lb (105.2 kcal/kg), respectively.

Using enthalpy change, [Equation (2)] the thermal duty is 11,023 × (189.4–63.3) = 1,390,000 Btu/h (350,000 kcal/h).

One can see that by using Equation (1) with an average specific-heat capacity and temperature change, the thermal duty is 1,123,500 Btu/h (283,150 kcal/h) or 81% of the true required duty determined by Equation (2). For such a case, a heat exchanger would be undersized by approximately 20% if the thermal duty using average specific heat was applied.

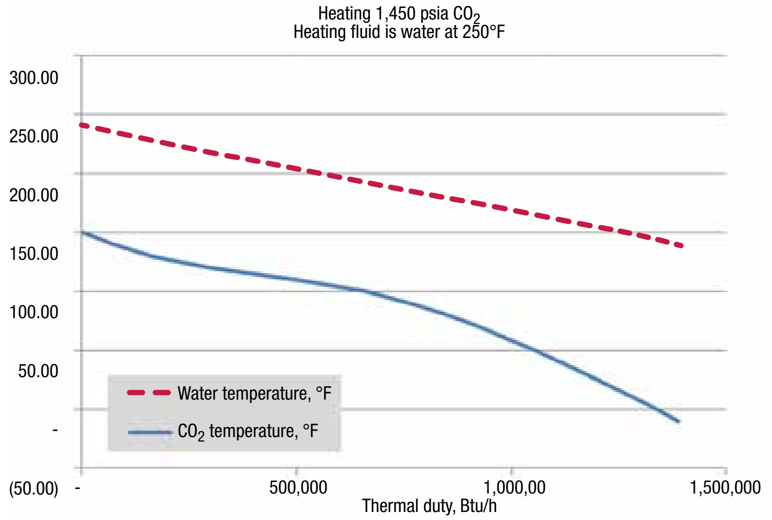


**FIGURE 3. This temperature versus thermal duty graph shows the non-linearity of $CO_2$ curve when heating $CO_2$ at a pressure of 1,450 psia**

## Temperature versus thermal duty

Best practice is to graph temperature change and heat release to understand the shape of the curve. Supercritical fluids can have surprisingly shaped curves caused by property variation as temperature changes. In many services, supercritical fluids will have nonlinear temperature versus thermal-duty curves, such as seen in Figure 3 [2]. This is especially relevant when operating conditions are between the critical pressure and pseudocritical pressure. First we should define these terms.

*Critical pressure* is the pressure above which a fluid is amorphous; that is, where there is not a distinction between liquid and gas phases, regardless of the temperature. *Pseudocritical pressure* and temperature is a point where the specific-heat capacity reaches a maximum value. There is great variation in specific heat capacity when, at a given pressure (isobar), the temperature approaches, reaches and surpasses the pseudocritical temperature. Let's return to Figure 3, which shows a supercritical-$CO_2$-heating application with water as the heating fluid. The temperature versus thermal-duty curve follows with $CO_2$ heated from –10°F to 150°F, and water cooled from 240°F to 140°F.

Notice that for $CO_2$, the shape of the curve is nonlinear. Common thinking is that the shape of the heating curve is linear, which is true for most sensible-heating applications. The nonlinear shape in supercritical fluid service is due to the large variation in enthalpy and, therefore, specific heat capacity as the $CO_2$ is heated. In this instance, the supercritical $CO_2$-heating curve bends into the water curve, thereby, reducing

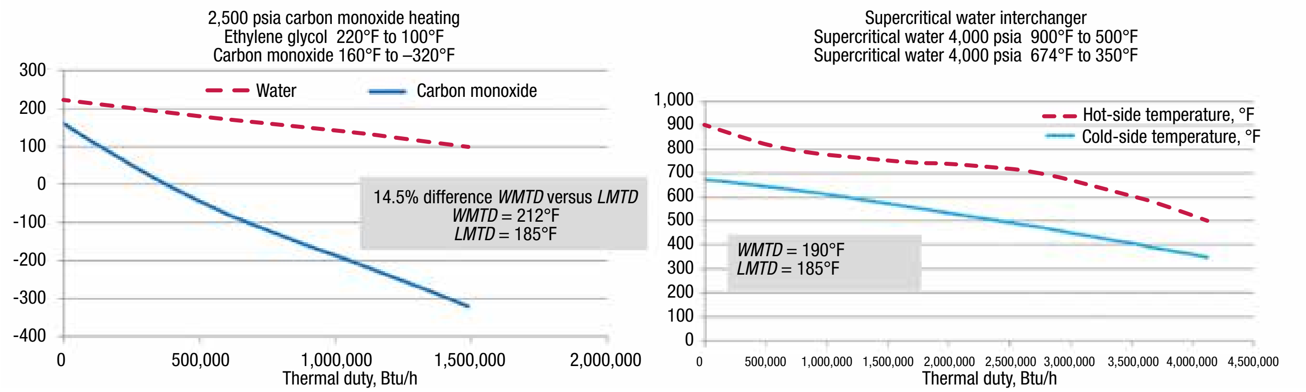


**FIGURE 4. Shown here are two examples of non-linear behavior of temperature versus thermal duty, and the resulting values calculated for *WMTD* and *LMTD***

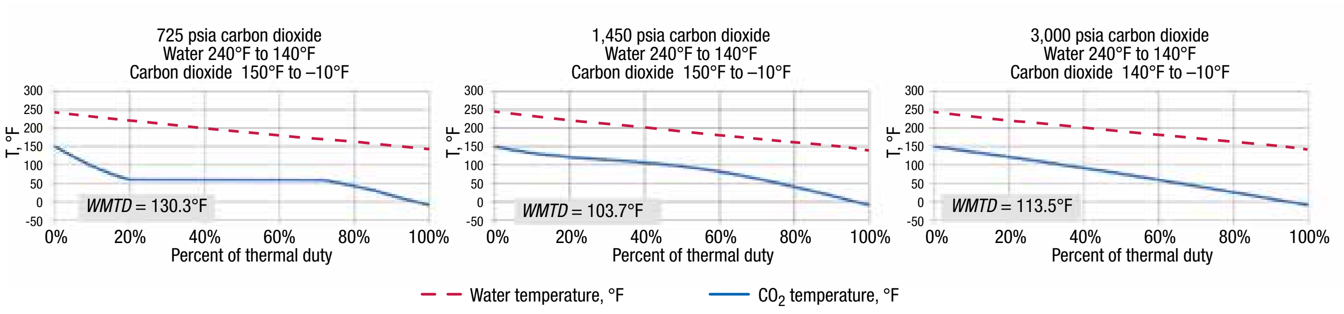


**FIGURE 5.** **Shown here are the heating curves for $CO_2$ at three different pressures**

the effective mean-temperature difference.

Conventional methods for countercurrent flow would determine the log mean-temperature difference (*LMTD*) using terminal temperature difference with a classic calculation as given by Equation (3)

$$LMTD = \frac{(240-150)-[140-(-10)]}{\ln\frac{(240-150)}{[140-(-10)]}} = 117.45°\text{F} \qquad (3)$$

Due to the shape of the $CO_2$ curve, a classic *LMTD* calculation will overstate the effective mean-temperature difference (MTD). In this example, it overstates MTD by 13%, as the next calculation shows.

Best practice is to apply a segmental approach, breaking the temperature curve into segments of smaller temperature changes and applying *LMTD* calculation for each step. This yields a duty-weighted, mean-temperature difference (*WMTD*), shown in Equation (4).

$$WMTD = \frac{Total\ thermal\ duty}{\sum_{segment\ i}^{segment\ n} \frac{Duty_i}{LMTD_i}} \qquad (4)$$

Using 10 segments, one for each 16 degree rise in $CO_2$ temperature, Equation (4) yields *WMTD* = 103.7°F.

For reliable performance and accurate heat-exchanger sizing, always consider using the *WMTD* calculation when the temperature profile is nonlinear.

Consider together thermal duty and *LMTD* and how dramatically different the heat-exchanger selection will be. When average specific heat is used, coupled with a classic *LMTD,* and that is compared to an enthalpy based thermal duty with a segmental *WMTD*, that concern for great care is apparent. Assuming the overall heat-transfer coefficient (*U*) is the same in either case, the required surface area differs by 40% (see Table 2).

Two additional examples comparing *WMTD* and *LMTD* are shown in Figure 4, which reinforces the risk associated with using the linear *LMTD* calculation and how the WMTD calculation yields a different number. The key take-away here is to plot the duty versus temperature and perform a segmented *WMTD* calculation to get it correct.

It is also interesting to compare the shape of the $CO_2$ heating curve for the very same temperature change from –10 to 150°F for three different isobars, as shown in Figure 5. A pressure of 725 psia is below the critical pressure. As the $CO_2$ is heated, there is sensible heating of liquid $CO_2$ up to the boiling temperature of 57.7°F. This is followed by isothermal boiling until all of the $CO_2$ is vaporized, and then gas sensible superheating to 150°F. In contrast, at a pressure of 3,000 psia, which is well above the critical pressure, the heating curve is close to linear and comparable to a sensible heating. For the 1,450-psia case, which is near to critical pressure, the shape of the heating curve is nonlinear and atypical.

## Fluid property variation

There can be wide variation in fluid properties, such as density, specific heat capacity, viscosity and thermal conductivity, between the inlet and the outlet temperature. Again, when operating between the critical pressure and the pseudocritical pressure, the specific heat may vary greatly with temperature. Good practice is to graph the fluid properties as a function of temperature to understand how extreme the variation might be. At a pressure well above the critical pressure and beyond the pseudocritical pressure, such a wide variation is reduced. Referring again to the 1,450 psia supercritical $CO_2$ example (Figure 5), the graph shown in Figure 6 depicts how fluid properties vary from an inlet temperature of –10°F to an outlet temperature of 150°F. Specific heat capacity stands out. Noteworthy is the pseudocritical point, which is 1,450 psia and approximately 110°F. Specific heat reaches a maximum at the pseudocritical point and is lower on either side of this point. The graph provides comparison for how properties vary up or down from properties determined at average temperature of 70°F (the average of –10°F and 150°F).

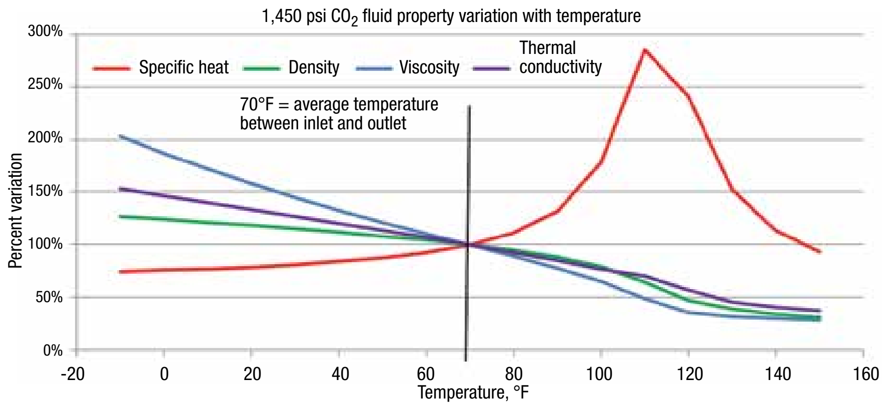


**FIGURE 6. Near the pseudocritical pressure, physical properties vary considerably as a function of temperature, especially the specific heat**

## Heat transfer coefficient

Supercritical fluids are often on the tubeside of a heat exchanger due to the high operating pressure, which is mechanically easier to contend with on the tubeside. Fluid properties directly influence the heat-transfer coefficient. When applying a classic Nusselt equation for in-tube flow at turbulent conditions, one can identify how a local heat-transfer coefficient is impacted by fluid properties, by the relationship between the Nusselt number, Nu, Reynold number, Re, and Prandtl number, Pr:

$$\mathrm{Nu} \propto \mathrm{Re}^{0.8} \times \mathrm{Pr}^{0.33} \quad (5)$$

Expression (5) reduces to Expression (6), which shows the relation between the tubeside heat-transfer coefficient, *HTC*, and the physical properties of viscosity, $\eta$, thermal conductivity, $\kappa$ and specific heat, $C_P$:

$$HTC \propto \eta^{-0.47} \times \kappa^{0.666} \times C_p^{0.333} \quad (6)$$

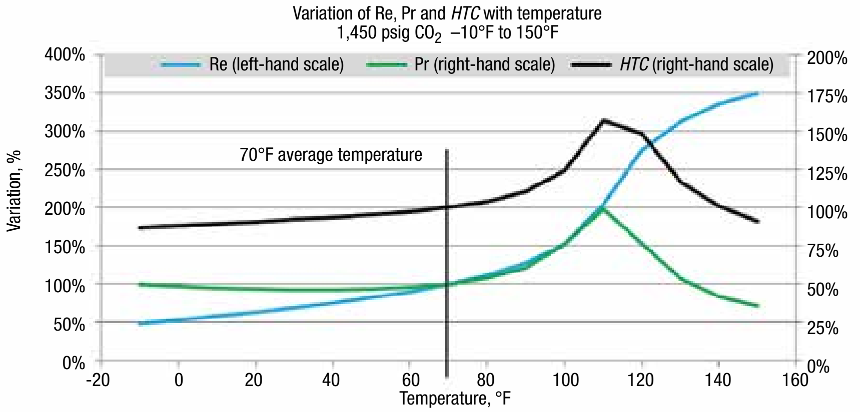


**FIGURE 7. The variation of Re, Pr and *HTC* as a function of temperature is shown here for $CO_2$ at 1,450°C**

From the graph shown in Figure 6, the specific heat variation greatly affects *HTC*, as does the viscosity and the thermal conductivity.

Research with supercritical fluids has found there can be significant radial property variation within a tube between average bulk temperature properties and those at the tube-wall temperature. There are factors one might apply to reflect the impact of bulk and tube-wall fluid properties for density, specific heat and viscosity.

Further to a segmental approach used to determine *WMTD*, it is recommended that *HTC* is considered segmentally as well to capture *HTC* variation along the temperature change. The graph shown in Figure 7 illustrates that, for 1,450 psig $CO_2$, the calculated *HTC* variance is 87% at the inlet, 157% near the pseudo-critical point and 90% at the outlet compared to the *HTC* determined at the average temperature of 70°F. This observation supports using a segmental approach (or discretization of temperature change) to capture cor-

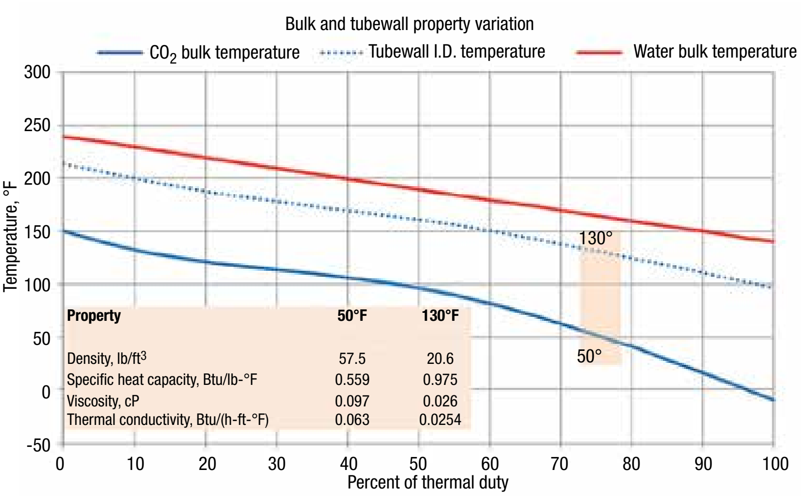


**FIGURE 8: This graph shows the variation of properties in the bulk and at the tubewall as a function of temperature**

rectly the local *LMTD* and *HTC*.

As noted previously, the bulk or average fluid properties can vary significantly from the fluid properties at the tube wall. Such variation will also influence *HTC*. The following equations are used for determining tubewall temperature on the inside (supercritical fluid side) and outside surface.

$$T_{wall_{ID}} = T_{TS} + \frac{U}{HTC}(T_{SS} - T_{TS})$$
(**7**)

$$T_{wall_{OD}} = T_{SS} + \frac{U}{H_{SS}}(T_{SS} - T_{TS})$$
(**8**)

Where:

$T_{wall,ID}$ = Tubewall temperature at the inside surface of the tube

$T_{wall,OD}$ = Tubewall temperature at the outside surface of the tube

$T_{TS}$ = Tubeside bulk temperature

$T_{SS}$ = Shellside bulk temperature

$U$ = Overall heat transfer coefficient

$HTC$ = Supercritical fluid heat-transfer coefficient

$H_{SS}$ = Shellside heat transfer coefficient

Let's return to the $CO_2$ heating application at 1,450 psig. By applying a segmental analysis with 10°F increments, we can compare the bulk or average temperature to the temperature of the tubewall inside diameter. There can be order-of-magnitude differences between bulk and tubewall properties when working with supercritical fluids. The graph shown in Figure 8 plots the tubewall temperature along the heat curve and illustrates how the fluid properties vary greatly between the bulk and those at wall temperature.

Some literature suggests using film-temperature properties. Film temperature is commonly considered to be the average of segment bulk and tubewall temperatures. Other literature applies correction factors for variation in specific heat and density. The author suggests applying physical properties that directionally drive the calculated *HTC* lower to provide a degree of safety. Film temperature serves as a good surrogate for determining what properties to apply. The author further suggests comparing bulk and film properties and using that property that yields a lower calculated *HTC*. If, however, the design provides adequate safety factors, such as, for example, a 60% cleanliness factor or a 50% excess area, then using film temperature for fluid properties is adequate.

Each supercritical fluid is unique, and the temperature-pressure region where a nonlinear thermal-duty curve is most likely will depend on a given fluids' properties. The closer the operating pressure is to the critical pressure, the more variation in specific heat as temperature changes is to be expected. Carbon dioxide has a critical pressure of 1,072 psia. Figure 9 illustrates how specific heat varies as temperature varies for different isobars. Note that the specific

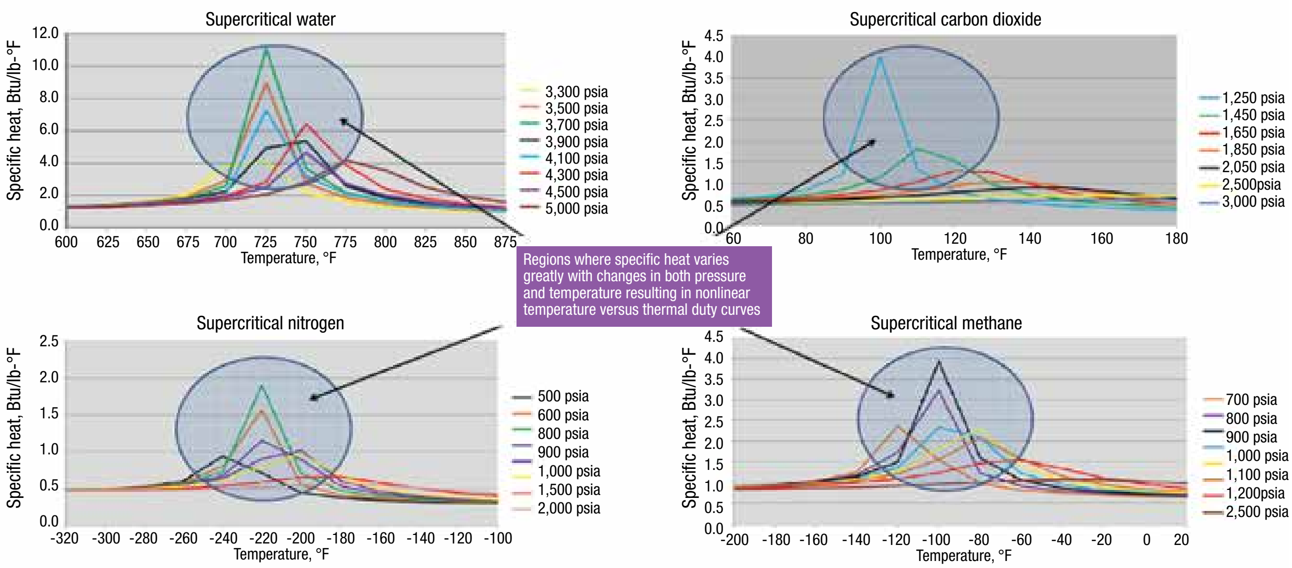


**FIGURE 9. These graphs show the variation of specific heat with temperature at several isobars for four different fluids. The shift of the pseudocritical temperature can be observed**

**TABLE 2. COMPARISON OF LINEAR VERSUS SEGMENTED CALCULATION**

| Parameter | Best practice | Risky practice |
|---|---|---|
| Thermal duty (*Q*), Btu/h | 1,390,000 ($\Delta h$-based) | 1,123,500 (*Cp*-based) |
| *MTD*, °F | 103.7 (segmented) | 117.5 (linear) |
| *Q*/*MTD* | 13,404 | 9,566 |
| Area, ft$^2$ (if $U = 100$) | 134 | 96 |

heat of 1,100 psia $CO_2$, which is just slightly greater than the critical pressure, is 29.72 Btu/lb°F when the temperature is 90°F. Recall a previous definition for pseudocritical temperature and pseudocritical pressure that describes where specific heat is a maximum. This is shown as the apex for each isobar in the graphs shown in Figure 9.

## Summary

Supercritical fluid heat transfer warrants more careful consideration than normally needed for more traditional heat-exchanger designs. This is due to fluid property variations when operating above the critical point and for a given isobar when the operating temperature is near to, or passes through the pseudocritical temperature. At a pressure well above the critical point there is less concern as property variation is not as significant. Key design considerations include the following:

- Determine the thermal duty of a supercritical fluid using enthalpy change
- Graph temperature versus thermal duty to understand shape of the curve
- When warranted, perform a segmental analysis to capture correctly *WMTD* and within each segment to determine surface area necessary based on segment thermal duty, segment *LMTD* and segment *HTC*
- Evaluate bulk and wall property variation to determine if further *HTC* refinement is necessary ■

*Edited by Gerald Ondrey*

## References


1. Van Wylen, Gordon J. and Sonntag, Richard E., "Fundamentals of Classical Thermodynamics," Wiley, Hoboken, N.J., 1993.
2. All fluid-property modeling used to generate the graphs was done using NIST REFPROP webbook, https://webbook.nist.gov/chemistry/name-ser.


## Author


**James R. Lines** is president and CEO of Graham Corp. (20 Florence Ave., Batavia, N.Y. 14020; Phone: 585-343-2216; Fax: 585-343-1097; Email: jlines@graham-mfg.com), a position he has held since 2008. Prior to that, Lines served as president and COO and as a director of the company. He has been working at the company in various capacities since 1984, holding positions of vice president and general manager, vice president of Engineering, and vice president of Sales and Marketing. Prior to joining the management team, he served as an application engineer and sales engineer as well as a product supervisor. Lines holds a B.S. in aerospace engineering from the State University of New York at Buffalo. The author's company has designed and successfully supplied its Heliflow heat exchangers in supercritical service for carbon monoxide, carbon dioxide, nitrogen, hydrogen, oxygen, methane, water and various other fluids.

Part 2

# ASTM Standards For Heat Transfer Fluids

This practical overview of ASTM standards can serve as a roadmap when selecting and evaluating heat transfer fluids

**Gerald E. Guffey II**
Eastman Chemical Co.

Heat-transfer-fluid systems are often used for process heating to 500°F or higher. To accomplish heating above 500°F, steam pressure must be above 600 psig. For many plants, distributing steam above 600 psig is impractical due to high cost and more stringent water-purity requirements. High-temperature heat-transfer fluids have a much lower vapor pressure than water at high temperature, so the design pressure of a heat-transfer-fluid system can be lower.

Most systems operate with the heat transfer fluid in the liquid phase. A few heat transfer fluids have a narrow boiling range and can be used in a vapor-phase system, but the design of the system is much different and the process heating temperature must match the boiling range of the fluid.

High-temperature heat-transfer fluids are generally classified as inorganic eutectic salts, synthetic organics (Figure 1), aromatic oils, paraffinic oils and silicone-based fluids. The chemistry of each heat-transfer fluid is different, so each fluid has different properties. Considerable background and technical information about heat transfer fluids is provided in chapter 21 of the ASTM Fuels and Lubricants Handbook. A new version of this handbook is expected to be published this month.

ASTM International (formerly known as the American Society for Testing and Materials; West Conshohocken, Pa.; www.astm.org) has developed several standards for heat transfer fluids other than inorganic eutectic salts. This article provides an overview of these standards. ASTM standards are listed using their ASTM designations, for example D5372. "D" indicates that the standard is administered by one of the D committees. "5372" is the number of the standard. These designations are used throughout this article.


**FIGURE 1. One type of synthetic organic heat transfer fluid is shown here**

## ASTM D5372 standard guide

ASTM D5372, "Standard Guide for Evaluation of Hydrocarbon Heat Transfer Fluids," covers the factors that should be considered to characterize a heat transfer fluid. These factors are also relevant to selection of a new heat-transfer fluid, so it can be used as a reference when choosing a new fluid. These factors are grouped into five categories: pumpability of the fluid, safety in use, effect on equipment, efficiency (heat-transfer capability) and service life.

***Pumpability.*** Several properties are relevant to the pumpability of a heat transfer fluid. Pumpability is briefly discussed in this standard, but it is discussed more extensively in D8046. Decreased flash point (measured by D92 or D93) is indicative of the presence of low-boiling compounds produced by thermal degradation of the fluid. Viscosity (measured by D445 or D7042) is a measurement of the fluid's resistance to flow. The presence of thermal degradation products can affect the viscosity of the fluid. As fluid temperature is decreased, at some point the fluid viscosity becomes too high to pump. There is some correlation between hydraulic shock during pumping with the fluid's specific gravity (measured by D1298 or D4052) and compressibility properties. Water in a heat-transfer-fluid system will vaporize and expand as system temperature is increased, building pressure. It is therefore important to keep water out of the system as much as possible. Water content can be measured using D95.

***Safety.*** Factors related to safety in use include autoignition temperature and flashpoint. Autoignition temperature can be measured using E659. The user should keep in mind that a hydrocarbon fluid absorbed on a porous inert surface (such as insulation) can ignite at temperatures more than 50°C lower than the value determined by E659. Flashpoint (measured by D92 Cleveland open cup tester or D93 Pensky-Martens closed cup tester) indicates the temperature at which flammable vapors given off by a liquid form a mixture with air that

can be ignited by contact with a hot surface, spark, or flame.

***Effect on equipment.*** Two ASTM standards can provide information about the effect of the heat transfer fluid on equipment. D471 provides data about the effect of the fluid on rubber or elastomeric seals. G4 is a guide for conducting corrosion tests in field applications.

***Efficiency.*** Several properties — thermal conductivity, specific heat, density and viscosity — are relevant to the heat transfer capability of the fluid. These are the properties used to calculate Reynolds number, Prandtl number and Nusselt number, which determine the heat transfer coefficient. D2717 measures thermal conductivity, D1298 or D4052 measures specific gravity, and D445 or D7042 measures viscosity. D2766, the test method listed for specific heat, has recently been withdrawn but E1269 and E2716 are other methods that could be considered.

***Service life.*** Heat transfer fluids degrade when exposed to sufficiently high temperature. The amount of degradation increases as temperature increases or exposure time increases. Thermal stability is measured using D6743.

Several tests are used to determine the condition of the fluid and its remaining service life. These tests include precipitation number (measured by D91), insoluble content (measured by D893), flash point (measured by D92 or D93), carbon residue (measured by D189, D524 or D4530), distillation (D86, D1160 and D2887 are listed but D2887 is more commonly used), neutralization number (measured by D664), color (measured by D1500), viscosity, viscosity index (measured by D2270) and water content (measured by D95). Typically, a sample of used heat-transfer fluid should be taken from each system at least once per year so that these tests can be conducted to evaluate fluid condition. To ensure that the sample is representative, it should be taken from the main circulating loop rather than from a dead leg. Some heat transfer fluid suppliers offer free evaluation of used fluid using these tests.

## ASTM D7665 standard guide

ASTM D7665, "Standard Guide for Evaluation of Biodegradable Heat Transfer Fluids," addresses biodegradable heat transfer fluids. It covers the same factors mentioned in D5372 but also includes a few others. Vapor pressure (measured by D2879) is included as a factor that influences pumpability of the fluid. Biodegradation (measured by D5864) is included as a factor to consider for safety in use. D6384, which covers terminology related to biodegradability and ecotoxicity of lubricants, is listed as a reference document. D7044, which is a specification for biodegradable fire-resistant hydraulic fluids, is also listed as a reference.

## ASTM D6743 standard test method

ASTM D6743, "Standard Test Method for Thermal Stability of Organic Heat Transfer Fluids," is a

test method that measures thermal stability of a heat transfer fluid. Thermal stability is the resistance to permanent change in fluid properties caused solely by heat. All heat-transfer fluids degrade with exposure to high temperature over time. Typically, the user wants their heat transfer fluid to last for many years. It's important to select a fluid that is thermally stable enough to last for many years at the expected system operating temperature.

The thermal degradation products for most heat transfer fluids include high- and low-boiling components, very low-boiling gases, and residue that cannot be evaporated. The presence of degradation products in the fluid affects its properties.

D6743 quantifies the high-boiling components, low-boiling components, very low-boiling gases, and residue that cannot be evaporated for a heat transfer fluid that is exposed to specified temperature for a specified time period. The test procedure consists of weighing heat transfer fluid into a stainless-steel ampoule, purging with nitrogen, sealing the ampoule, and heating it in an oven. After the ampoule is removed from the oven and cooled, the fluid is analyzed to quantify the amount of thermal degradation products produced. Measurement of thermal degradation products is done by gas chromatography (GC), distillation and weighing.

Before D6743 was developed, each heat-transfer-fluid manufacturer had its own method for determining thermal stability. There were differences in the methods, as well as differences in the equipment used to conduct them. These differences sometimes led to conflicting test results. One supplier's test data might indicate that fluid A was more thermally stable than fluid B, while another supplier's test data might show the opposite.

D6743 provides a standard test method for developing data that a user can evaluate to compare heat transfer fluids. Using D6743, thermal stability of two or more different heat-transfer-fluid chemistries can be directly compared by heating them at the same time in the same oven, and then analyzing them using the same equipment. D6743 is very specific about the type of equipment that can be used. For example, it specifies the type and length of the GC column, film type and thickness, type of detector, calibrant range, material and dimensions of the ampoule, temperature control capability of the oven, and accuracy of the balance for weighing. Statistical analysis of test data from one laboratory showed very good repeatability of test results (see the precision and bias statement in the method).

DIN (Deutsches Institute für Normung e.V.; Berlin, Germany; www.din.de) also has a test method for thermal stability, but it is less specific about the test equipment that can be used. Differences in test equipment used can cause significant differences in test results.

## LIST OF ASTM STANDARDS REFERENCED IN THIS ARTICLE

| | |
|---|---|
| **D5372** | Standard Guide for Evaluation of Hydrocarbon Heat Transfer Fluids |
| **D93** | Standard Test Methods for Flash Point by Pensky-Martens Closed Cup Tester |
| **D445** | Standard Test Method for Kinematic Viscosity of Transparent and Opaque Liquids (and Calculation of Dynamic Viscosity) |
| **D7042** | Standard Test Method for Dynamic Viscosity and Density of Liquids by Stabinger Viscometer (and the Calculation of Kinematic Viscosity) |
| **D1298** | Standard Test Method for Density, Relative Density, or API Gravity of Crude Petroleum and Liquid Petroleum Products by Hydrometer Method |
| **D4052** | Standard Test Method for Density, Relative Density, and API Gravity of Liquids by Digital Density Meter |
| **D95** | Standard Test Method for Water in Petroleum Products and Bituminous Materials by Distillation |
| **E659** | Standard Test Method for Autoignition Temperature of Chemicals |
| **D92** | Standard Test Method for Flash and Fire Points by Cleveland Open Cup Tester |
| **D471** | Standard Test Method for Rubber Property—Effect of Liquids |
| **G4** | Standard Guide for Conducting Corrosion Tests in Field Applications |
| **D2717** | Standard Test Method for Thermal Conductivity of Liquids |
| **D6743** | Standard Test Method for Thermal Stability of Organic Heat Transfer Fluids |
| **D91** | Standard Test Method for Precipitation Number of Lubricating Oils |
| **D893** | Standard Test Method for Insolubles in Used Lubricating Oils |
| **D189** | Standard Test Method for Conradson Carbon Residue of Petroleum Products |
| **D524** | Standard Test Method for Ramsbottom Carbon Residue of Petroleum Products |
| **D4530** | Standard Test Method for Determination of Carbon Residue (Micro Method) |
| **D86** | Standard Test Method for Distillation of Petroleum Products and Liquid Fuels at Atmospheric Pressure |
| **D1160** | Standard Test Method for Distillation of Petroleum Products at Reduced Pressure |
| **D2887** | Standard Test Method for Boiling Range Distribution of Petroleum Fractions by Gas Chromatography |
| **D664** | Standard Test Method for Acid Number of Petroleum Products by Potentiometric Titration |
| **D1500** | Standard Test Method for ASTM Color of Petroleum Products (ASTM Color Scale) |
| **D2270** | Standard Practice for Calculating Viscosity Index from Kinematic Viscosity at 40 °C and 100 °C |
| **D7665** | Standard Guide for Evaluation of Biodegradable Heat Transfer Fluids |
| **D2879** | Standard Test Method for Vapor Pressure-Temperature Relationship and Initial Decomposition Temperature of Liquids by Isoteniscope |
| **D5864** | Standard Test Method for Determining Aerobic Aquatic Biodegradation of Lubricants or Their Components |
| **D6384** | Standard Terminology Relating to Biodegradability and Ecotoxicity of Lubricants |
| **D7044** | Standard Specification for Biodegradable Fire Resistant Hydraulic Fluids |
| **D7863** | Standard Guide for Evaluation of Convective Heat Transfer Coefficient of Liquids |
| **D8046** | Standard Guide for Pumpability of Heat Transfer Fluids |
| **E794** | Standard Test Method for Melting And Crystallization Temperatures By Thermal Analysis |
| **D2983** | Standard Test Method for Low-Temperature Viscosity of Automatic Transmission Fluids, Hydraulic Fluids, and Lubricants using a Rotational Viscometer |
| **D891** | Standard Test Methods for Specific Gravity, Apparent, of Liquid Industrial Chemicals |
| **D6304** | Standard Test Method for Determination of Water in Petroleum Products, Lubricating Oils, and Additives by Coulometric Karl Fischer Titration |

### ASTM D7863 standard guide

ASTM D7863, "Standard Guide for Evaluation of Convective Heat Transfer Coefficient of Liquids," provides information about the calculation of convective heat-transfer coefficient. The factors that affect calculation of convective heat-transfer coefficient are described. Results from previous studies have been presented in different ways, so direct comparison of convective heat-transfer-coefficient data from these studies can be challenging. Therefore, this guide focuses on describing a standard approach for obtaining data, interpreting data, and presenting results.

This guide describes a test equipment arrangement with turbulent fluid flow inside an electrically heated tube that has a wall temperature higher than the bulk fluid temperature. Features of this test-equipment arrangement are discussed and the required measurements are defined. The ASTM test methods recommended for making each of the required measurements are listed. Considerations for calibration of the test equipment are discussed. Formulas used to calculate the heat-transfer coefficient are summarized. Appropriate ways to interpret, present and report the test results are explained.

### ASTM D8046 standard guide

ASTM D8046, "Standard Guide for Pumpability of Heat Transfer Fluids," discusses the fluid properties and system configuration issues that affect the ability to pump a heat transfer fluid. These properties include flashpoint (measured by D92 or D93), crystallization temperature (measured by E794), viscosity (measured by D445, D2983 or D7042), relative density (measured by D891 or D4052), water content (measured by D6304), vapor pressure (measured by D2879), and boiling range distribution (measured by D2887). System configuration issues include the type of pump used, mechanical seals, the pump suction piping arrangement, net positive-suction head required by the pump, and electric motor sizing. The need to consider how fluid viscosity will change as the fluid degrades and how that affects pump and motor selection is also discussed. This guide addresses several considerations about pumping that are a useful reference when selecting a new heat-transfer fluid. ■

*Edited by Gerald Ondrey*

### Author

**Gerald Guffey** is a senior associate engineer in the Worldwide Engineering and Construction Division of Eastman Chemical Co. (100 Eastman Road, Kingsport, TN 37660; Phone: 423-229-1095; Email: gguffey@eastman.com). He has been involved in design and evaluation of heat transfer fluid systems and fired heaters for more than twenty years. He has been a member of ASTM since 1997. He holds a Bachelor of Science degree in Mechanical Engineering from Georgia Tech.

# Preparing for a Successful Security Audit

## Facing a site security audit might seem daunting, but proper preparation will help to meet the goals of enhancing security and reducing risk

**Ronald Razzolini**
**Telgian Management Technologies**

What are the downsides of failing to pass a security audit or inspection? Is it the fear of reputational damage for not passing? Is it the added scrutiny and attention your location will receive from the corporate office? Will it result in a regulatory enforcement action by a governmental agency? Or will you fail to recognize a gap — a deficiency — in a component of your overall security systems plan? Such a gap could expose your business and employees to regulatory enforcement action or even worse — to intrusion, theft, harm or other subversive activity.

Passing a security inspection or audit should be an easy and straightforward process, provided that it is approached in an organized manner. The "5 Ps" adage — "proper planning prevents poor performance" — should be an organization's background theme for the inspection. Furthermore, an added benefit is that the preparation and organizational activities you undertake ahead of time can help identify even the minor items that are often unforeseen gaps in your security plan. This article breaks down the security inspection or systems audit into five distinct components, and provides guidance for successful execution during each phase of the process (Figure 1).


**FIGURE 1.** A site security audit or inspection might seem intimidating at the outset, but proper preparation with a team of skilled personnel will help put things into perspective

### Before the inspection

Proper planning is the top priority before the inspection. The time spent in preparation ahead of time will pay off during the inspection, including the assembly of the team. This team should include the security director and the facility manager, as well as their assistants, if these roles are filled. If there are cyber assets at the site, include the person in charge of them (Figure 2). If a corporate information technology (IT) or cyber systems manager oversees cyber activities from a different location and cannot attend in person, have them be available for a planning conference call. The same holds for human resources representatives.

Lay out the expectations for the inspection with your team. Clearly explain that everyone is expected to play a part in the inspection. This will demonstrate to the inspection team that your staff is actively engaged in the process. Do not give the impression that security is a one-person show. Instruct the team to answer any questions posed by the inspectors clearly and truthfully. Never guess if you do not know the answer, and when you are done answering a question, do not keep talking. It is important to avoid speculation and rambling thoughts.

Every inspection involves a review of documents. Some examples are procedures, impairment reports, incident reports, training records and even personnel records. Rather than collecting these items immediately before the inspection, employ a system where you can capture the necessary documents in real time as you use or generate them.

Work with your team to plan out the areas of the site that will be part of the inspection tour. Walk the route with your team, note any relevant security items in place and any that may be lacking or in need of attention. Assign responsibility for correcting any items that need attention. In the same light, note any improvements or additions made that enhance your posture. Write them down in your notes and be sure to share with the inspectors during the actual tour.

After the team completes the planning site walkthrough, reconvene as a group and go over everyone's notes and comments. If you have any outstanding action items, spell them out. Determine who will take responsibility for them and when they will be completed.

If a required practice or piece of security equipment is on the "to be repaired" list, but will not be returned to fully operational status before inspection time, enact your impairment plan that addresses the shortfall. If you do not have an impairment


**FIGURE 2.** Digital assets are an important facet of overall site security, so audit planning teams should include the appropriate cybersecurity personnel

plan that addresses the issue, develop one with your team, put it into operation and document it.

Notify site personnel and site security staff once the inspection has been scheduled, when it will occur, and by whom it will be conducted.

## Inspection day

The inspection day can be broken down into the following four segments:

- Opening meeting
- Site walkthrough
- Document review and interviews
- Closing meeting

If the inspection is set to cover multiple days, these segments, with the exception of the closing meeting, may be intermixed in each day or could follow in sequential order. Be flexible, and remember the "5 Ps" approach described previously. Here is where it will greatly pay off.

## Opening meeting

You never get a second chance to make a first impression, so start off on the right foot during the opening meeting. Welcome the inspection team and thank them for their attention. Up front, cover any "housekeeping" items, including the following:

- Site safety requirements, including required personal protective equipment (PPE)
- Agenda and timing; for instance, an outline or agenda from the inspector
- Locations of restrooms, telephones and how to access wireless connectivity, if needed
- Allow your team to introduce themselves and describe what role they play at the site, and in the inspection
- Allow the inspection team to introduce themselves and state their roles
- Readdress the intent of the inspection. If the site tour covers a large area, consider showing an overhead image of the area. Point out key areas. If it is within a large building, such as a warehouse, consider using a floorplan drawing. Again, remember to point out the key areas

If this is the inspection team's first visit to the location, give an overview of the site. Items to include are products produced, services provided, number of personnel employed and company history. Be certain to allow the inspection team leader the opportunity to speak about their objectives and plans.

## Site walkthrough

For a small group, do not overwhelm one or two inspectors with a dozen people from your team. Have your key team members with you and ask area-specific personnel that may be needed during the inspection to meet you when the tour reaches their location.

If there are a number of inspectors, and the plan is to break into groups, be sure to assign the appropriate personnel from your team to each group.

Follow the route you planned that covers the areas to be inspected. Do not stray or wander. If there is any work or maintenance-type activity that could pose a hazard in a certain area, use flagging tape to section it off. Be sure to point out that there is work going on in that area and explain why you are not entering the area.

Make a note of key security items or components. If a key item is out of service, be sure to point this out, coupled with highlighting the impairment activity you have underway to address the shortfall. Let the inspectors see that you are proactive and show them the impairment plan in action.

Team members should focus on the tour and the questions from the inspectors. They should not engage in sidebar or personal conversations amongst themselves. Likewise, they should answer questions pertinent to their area of responsibility. Remember, it is not a one-person event. Appoint someone from your team to act as the "sweeper" for each group on the tour. Their job is to round up any wanderers and keep the group together and orderly.

Make a written note of any questions asked that are to be addressed during the interview portion of the inspection. If the inspection requires photographs to be taken by the inspectors, be sure to take an identical photo with a company-supplied camera. This can be especially helpful if a question about something viewed comes up at a later date.

## Document review and interview

Typically, the inspector, or inspection team leader, takes the lead during the document review and interview phase. Be prepared to answer questions regarding items or activities seen on the tour. Again, answer clearly, truthfully and to the point of the question. When you have clearly answered the question, stop talking. If you do not know the answer, do not guess, speculate or make something up. Offer to find the answer, make note of the issue, and be certain to follow through. If an immediate answer is required, take a break and locate the information needed to satisfy the question.

The team leader must ensure good communication. If you do not understand a question, it is not out of line to ask for clarification. Similarly, be sure that the message that you and your team are conveying is clear and is understood by the inspector. Avoid using acronyms, nicknames or local site jargon that may mean something to you and your team, but are terms unfamiliar to those not from the site. Along the same lines, if an answer involves a discussion of a more technical nature, ensure the inspector understands what you are

**FIGURE 3.** Prior to the site security inspection, gather any required documents and be sure that the appropriate parties are given duplicate copies

trying to convey.

Any documents that are required to be reviewed should be on hand (Figure 3). If electronic versions are allowed, as opposed to written copies, have the necessary computers at the ready. The same follows for any required projection equipment. In your pre-inspection planning, you should have ensured that the most current version of any procedure, inspection report, maintenance log and so on is the version you have on hand.

If the inspector requires a copy of any document, be certain to note which document that is and be sure to retain a copy of the document they received. If notations were made to any photographs taken, be certain to add those notations to any duplicate photos in your possession.

## Closing meeting

The closing meeting should include the same personnel that participated in the opening meeting. Generally, the closing meeting is led by the inspector or inspection team lead. They may note items that they felt are commendable and some that are even unique and noteworthy. Similarly, they will bring up areas or items that are not in accordance with requirements or for which they have further questions. If something was misinterpreted by the inspector, take the opportunity to politely clarify the issue and bring it to a resolution.

Be sure to recap any "to do" items noted during the inspections process, including followup action items, documents or images to be sent to the inspector or other promises made. These should all be recapped in the closing meeting, along with who owns the task and the date of delivery that was committed to. When delivery of these items is completed, document it.

Be certain to ask if there are any open issues or items. Take time to review your notes from the site tour to ensure any questions or items you captured on the tour have not been overlooked. Also, make an effort to note any followup or next-step actions to be completed. Thank the inspectors and thank your team.

When all is said and done, you should be able to look back and see that the organization of your records, as well as the planning and preparation that you and your team put into place before the inspection, yielded a smooth inspection and a positive outcome.

If you found yourself struggling to answer questions and locate documents, or not having every member of your team involved in the process, use the lessons learned to build a more robust document-retention program. Going forward, make efforts to work with your staff to become better organized and address the issues collectively. Build on the strengths of the group as a combined unit instead of individual efforts. Use the experience to not only strengthen your security posture, but also your management process. It will prove to be quite valuable in the long term. ■

*Edited by Mary Page Bailey*

## Author

**Ronald Razzolini** is the director of business development at Telgian Management Technologies (4001 Kennett Pike, Ste. 308, Wilmington, DE 19807; Email: rrazzolini@telgian.com). His experience includes over 35 years in chemical sector safety and a deep technical knowledge of safety and compliance programs and procedures. Razzolini also plays an integral role in chemical safety and security procedure development nationwide. His committee experience includes the American Chemistry Council Chemical Security Committee (2001–2018), where he acted as committee chairman from 2010 to 2013. This working group was chartered to protect the chemicals sector from threats of terrorism and coordinate activities among industry, legislators and the U.S. Department of Homeland Security. Razzolini also participated on the National Infrastructure Advisory Council, where he acted as a subject-matter expert on projects addressing information sharing between federal intelligence agencies and the private sector. Prior to joining Telgian Management Technologies, he was the corporate director of safety/security at PVS Chemicals, Inc. in Detroit for almost 20 years. Razzolini is a graduate of Medaille College in Buffalo, N.Y. with a B.S. in business administration.

# Economic Indicators

**2017** ▬ **2018** ▬ **2019** ▬

**Download the CEPCI two weeks sooner at www.chemengonline.com/pci**

## CHEMICAL ENGINEERING PLANT COST INDEX (CEPCI)

| (1957–59 = 100) | Aug. '19 Prelim. | July '19 Final | Aug. '18 Final |
|---|---|---|---|
| *CE* Index | 602.1 | 604.6 | 614.6 |
| Equipment | 731.7 | 735.8 | 749.8 |
| Heat exchangers & tanks | 639.7 | 646.8 | 669.3 |
| Process machinery | 723.8 | 722.2 | 728.1 |
| Pipe, valves & fittings | 954.1 | 953.9 | 979.8 |
| Process instruments | 412.9 | 415.4 | 421.2 |
| Pumps & compressors | 1071.6 | 1068.2 | 1029.1 |
| Electrical equipment | 559.6 | 558.3 | 539.7 |
| Structural supports & misc. | 781.6 | 796.4 | 826.6 |
| Construction labor | 337.6 | 335.6 | 336.5 |
| Buildings | 591.8 | 593.9 | 602.5 |
| Engineering & supervision | 313.9 | 314.3 | 317.6 |

Starting in April 2007, several data series for labor and compressors were converted to accommodate series IDs discontinued by the U.S. Bureau of Labor Statistics (BLS). Starting in March 2018, the data series for chemical industry special machinery was replaced because the series was discontinued by BLS (see *Chem. Eng.*, April 2018, p. 76–77.)

Annual Index:

2011 = 585.7

2012 = 584.6

2013 = 567.3

2014 = 576.1

2015 = 556.8

2016 = 541.7

2017 = 567.5

2018 = 603.1

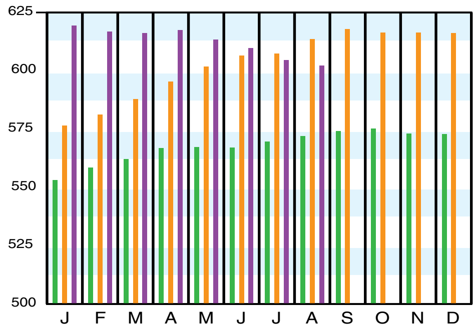


## CURRENT BUSINESS INDICATORS

| | LATEST | | | PREVIOUS | | | | | | YEAR AGO | | |
|---|---|---|---|---|---|---|---|---|---|---|---|---|
| CPI output index (2012 = 100) | Sept. '19 | = | 102.1 | Aug.'19 | = | 102.7 | Jul.'19 | = | 101.5 | Sept. '18 | = | 103.3 |
| CPI value of output, $ billions | Aug.'19 | = | 1,965.0 | Jul.'19 | = | 1,976.6 | Jun.'19 | = | 1,966.1 | Aug. '18 | = | 2,001.2 |
| CPI operating rate, % | Sept. '19 | = | 76.0 | Aug.'19 | = | 76.5 | Jul.'19 | = | 75.7 | Sept. '18 | = | 77.8 |
| Producer prices, industrial chemicals (1982 = 100) | Sept. '19 | = | 239.8 | Aug.'19 | = | 248.3 | Jul.'19 | = | 256.3 | Sept. '18 | = | 283.9 |
| Industrial Production in Manufacturing (2012 =100)* | Sept. '19 | = | 104.8 | Aug.'19 | = | 105.2 | Jul.'19 | = | 104.7 | Sept. '18 | = | 105.7 |
| Hourly earnings index, chemical & allied products (1992 = 100) | Sept. '19 | = | 184.4 | Aug.'19 | = | 185.1 | Jul.'19 | = | 184.9 | Sept. '18 | = | 185.2 |
| Productivity index, chemicals & allied products (1992 = 100) | Sept. '19 | = | 96.3 | Aug.'19 | = | 96.8 | Jul.'19 | = | 95.6 | Sept. '18 | = | 97.9 |

### CPI OUTPUT INDEX (2000 = 100)†

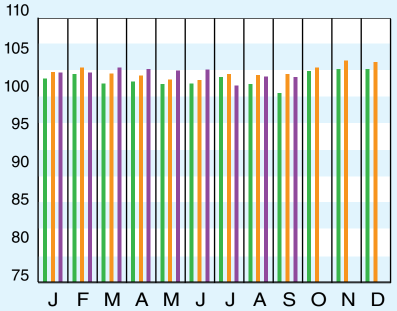


### CPI OUTPUT VALUE ($ BILLIONS)

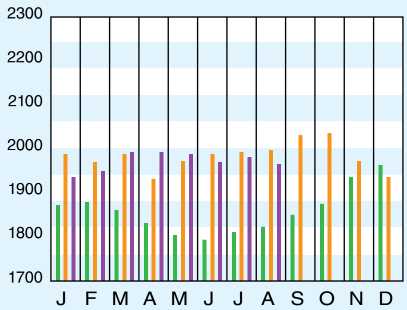


### CPI OPERATING RATE (%)

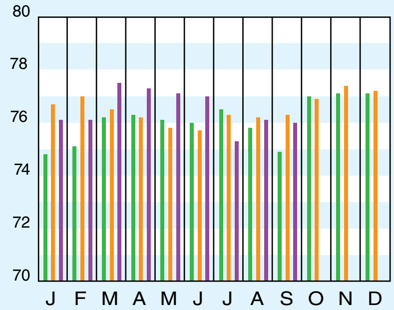


*Due to discontinuance, the Index of Industrial Activity has been replaced by the Industrial Production in Manufacturing index from the U.S. Federal Reserve Board.
†For the current month's CPI output index values, the base year was changed from 2000 to 2012
Current business indicators provided by Global Insight, Inc., Lexington, Mass.

### CURRENT TRENDS

The preliminary value for the *CE* Plant Cost Index (CEPCI; top; the most recent available) for August 2019 decreased from the previous month's value. The decline is the sixth within the last seven months. While the Construction Labor subindex rose in August, the other three subindices — Equipment, Buildings and Engineering & Supervision — decreased, giving rise to the decline in the overall CEPCI. The preliminary August CEPCI value is 2.0% lower than the corresponding value from a year ago. The magnitude of the difference in the year-on-year values increased from the previous month. Meanwhile, the CBI numbers for September 2019 (middle) show a small decrease in the CPI Output Index.